from R & D System (Minneapolis, USA). Human parathyroid hormone 1–34 (PTH 1–34) was obtained from Peptide Institute (Osaka, Japan). Antibodies used for immunohistochemistry include a monoclonal antibody directed against human von Willebrand factor (vWF) (Dako, Glostrup, Denmark), a monoclonal antibody for human thymidine glycol (TG) (Japan Institute for the Control of Aging, Shizuoka, Japan), a polyclonal antibody targeting human M-CSF (Santa Cruz Biotechnology, Santa Cruz, CA) and a monoclonal antibody against vitronectin receptors (VNRs; human CD51/61 complex) (23C6) (Serotec, Oxford, UK).

Cell culture and osteoclast formation assay

CD14+ monocyte like cells were isolated from heparinized peripheral blood from seven healthy volunteers using anti-CD14 antibody-coated beads (Myltenyi Biotec GmbH, Germany) as described previously [16]. SaOS-4/3 cells were established from a human osteosarcoma cell line (SaOS-2) by stable transfection with human PTH/PTHrP receptor cDNA [17]. SaOS-4/3 cells support the development of human osteoclasts after stimulation by parathyroid hormone (PTH) [17,18].

For monoculture, CD14+ cells were grown in α-minimum essential medium (αMEM; Gibco BRL, Gaithersburg, MD) supplemented with 10% fetal calf serum (FCS; Hyclone, Logan, UT) in the presence of M-CSF (25 ng/ml) and RANKL (40 ng/ml). Cells were cultured under a normal oxygen tension (normoxia; 20% O_2 and 5% CO_2) or under a high oxygen tension (hyperoxia; 40% O_2 and 5% CO_2), or under a switching oxygen tension from normoxia to hyperoxia after cells began to form multinucleation, (normoxia→hyperoxia; N→H). The culture medium was exchanged every 3 days.

For coculture, CD14+ cells (3×10^4/well) were incubated with SaOs-4/3 cells (5×10^3/well) in the presence of PTH (10^{-8} M) in αMEM supplemented with 10% fetal calf serum under normoxic, hyperoxic, or N→H conditions.

After the indicated period, cells were fixed and stained for tartrate-resistant acid phosphatase (TRAP) with a TRAP staining kit (Hokudo, Hokkaido, Japan) to evaluate osteoclast formation, as described previously [16]. The number of TRAP-positive multinuclear cells with more than 3 nuclei and TRAP-positive mononuclear cells was counted every week. For immunohistochemical staining, cells were fixed with cold methanol: acetone (50: 50, volumetric ratio) for 10 min and incubated with a monoclonal antibody against VNRs, an osteoclast-associated antigen. The bound antibodies were visualized with biotinylated secondary antibodies, avidin–biotin-conjugated peroxidase, and an aminoethylcarbazole substrate kit (Histofine; Nichirei, Tokyo, Japan). Osteoclastogenesis assay were repeated using CD14+ cells of at least three donors. All experiments were triplicated.

Reverse transcription-polymerase chain reaction (RT-PCR)

Total RNA was extracted from 5×10^6 CD14+ cells with an RNeasy Kit (Qiagen, Hilden, Germany) according to the manufacturer's directions. After treatment with DNase I (Life Technologies, Rockville, MD), single-stranded cDNA was synthesized using 2 μg of each RNA sample, 100 ng of random primers, and 4 U of Omniscript Reverse Transcriptase (Qiagen) in a total reaction volume of 20 μl. Amplification was performed with 0.5 U of TaKaRa Ex Taq (Takara, Shiga, Japan). In all cases, reproducibility was confirmed by at least triplicate experiments. The primers for RANK, M-CSF, RANKL, OPG, and GAPDH have been described previously [16]. The other primer sets for DC-STAMP, Bim, Bcl2, and c-fms are shown in Table 1.

Quantitative real-time PCR

We obtained cDNA by reverse transcription as mentioned above, and proceeded to perform real-time PCR using the Roche Applied Science Light Cycler system (Roche, Basel, Switzerland). The SYBR Green assay (Roche), in which each cDNA sample was evaluated in triplicate with 20-μl reaction mixtures, was employed for all target transcripts. Expression was normalized by comparison with that of GAPDH.

Western blot analysis of M-CSF

To detect M-CSF protein, SaOs-4/3 cells were cultured for 3 or 14 days under normoxic or hyperoxic conditions. Western blot analysis was performed using whole cell lysates and 20-μl aliquots of each sample were applied. The blots were incubated with monoclonal or polyclonal antibodies for human M-CSF and then with horseradish peroxidase-coupled anti-mouse or anti-rabbit antibodies (Amersham Biosciences).

Assay of M-CSF

The M-CSF level in the conditioned medium (days 1–3, 4–6, 7–9, 10–12, and 13–16) harvested from cultures of SaOs-4/3 cells incubated under normoxic or hyperoxic conditions was measured with a human M-CSF ELISA kit (RayBiotech, Inc. Norcross, GA, USA) according to the manufacturer's instructions. Results were normalized by the number of SaOs-4/3 cells.

Inhibition of M-CSF with a neutralizing antibody

CD14+ cells (3×10^4 cells/well) were incubated with SaOs-4/3 cells (5×10^3 cells/well) in the presence of PTH (10^{-8} M) in αMEM supplemented with 10% fetal calf serum under normoxic or hyperoxia in 96-well plates for 24 h. Then neutralizing antibodies against human M-CSF were added to the cocultures after day 1 (final concentrations; 0 ng/ml=control, 50 ng/ml, 500 ng/ml), and day 14 or 25 (final concentration; 500 ng/ml). The culture medium was replaced every 3 days with the fresh medium. The number of TRAP-positive multinuclear cells with more than 3 nuclei was counted every week.

Histological examination of tissue samples

Tissue samples that included the bone-synovial interface were obtained during total knee arthroplasty from three RA patients and three osteoarthritis (OA) patients after informed consent was provided. The American College of Rheumatology criteria were used for the diagnosis of RA [19]. Tissue samples were fixed in 4%

Table 1
Sequences of polymerase chain reaction primers

	Primers (5′–3′)		Product size (bp)
	Sense	Antisense	
DC-STAMP	5′GGCCAGTGCCAAGCAGGACGAG3′	5′GCAGCTGGCACAGGGATCGTCA3′	388
Bim	5′GCAGCCGAAGACCACC3′	5′ACCGCGGTGCTGGGTC3′	151
Bcl2	5′AGCATCAGGCCGCCACAAG3′	5′CTGGAGGGCCCCAGGGTGA3′	239
c-fms	5′-TGCTGCTCCTGCTGCTATTG-3′	5′-TCAGCATCTTCACAGCCACC-3′	270

DC-STAMP = dendritic cell specific transmembrane protein.

paraformaldehyde at 4 °C for 24 h, and decalcified in 20% EDTA for 2 weeks. Next, the samples were dehydrated through an ethanol series and embedded in paraffin. Sections (4 μm thick) were cut on a microtome for TRAP and immunohistochemical analysis. The streptavidin–biotin–peroxidase complex technique with a Histofine SAB-PO kit (Nichirei) used for immunohistochemical staining. Briefly, after blocking endogenous peroxidase and nonspecific antigens, tissue sections were incubated with primary antibodies against VW, M-CSF, and TG for 24 h at 4 °C. The sections were washed with phosphate buffered saline and incubated with the secondary antibody, following by peroxidase-conjugated streptavidin (Nichirei). After a wash with phosphate buffered saline, the sections incubated with 3,3′-diaminobenzidine tetrahydrochloride (Dojindo, Kumamoto, Japan) to detect peroxidase activity.

Statistical analysis

Results are expressed as the mean±standard deviation (SD). Differences between groups were assessed by Student's *t*-test, and differences among three or more groups were assessed by post hoc analysis (Turkey–Kramer and Fisher protected least significant difference test). A p value <0.05 was considered statistically significant.

Results

TRAP-positive cells in hyperoxic and normoxic culture

To confirm osteoclast formation, we performed TRAP staining and counted the positive cells. As shown in Fig. 1A, TRAP-positive cells appeared in cultures of CD14+ cells at day 6 and the number of positive cells under hyperoxia was the same as under normoxic conditions until 14 days. In CD14+ cells monoculture with N→H, there was no effect of hyperoxia. The results obtained with vitronectin receptor (VNR) staining were the same as those for TRAP staining (data not shown). We counted the number of TRAP-positive multinuclear cells with more than 3 nuclei. There was no difference in number of these cells between two oxygen conditions (Fig. 1A-2). Next, CD14+ cells

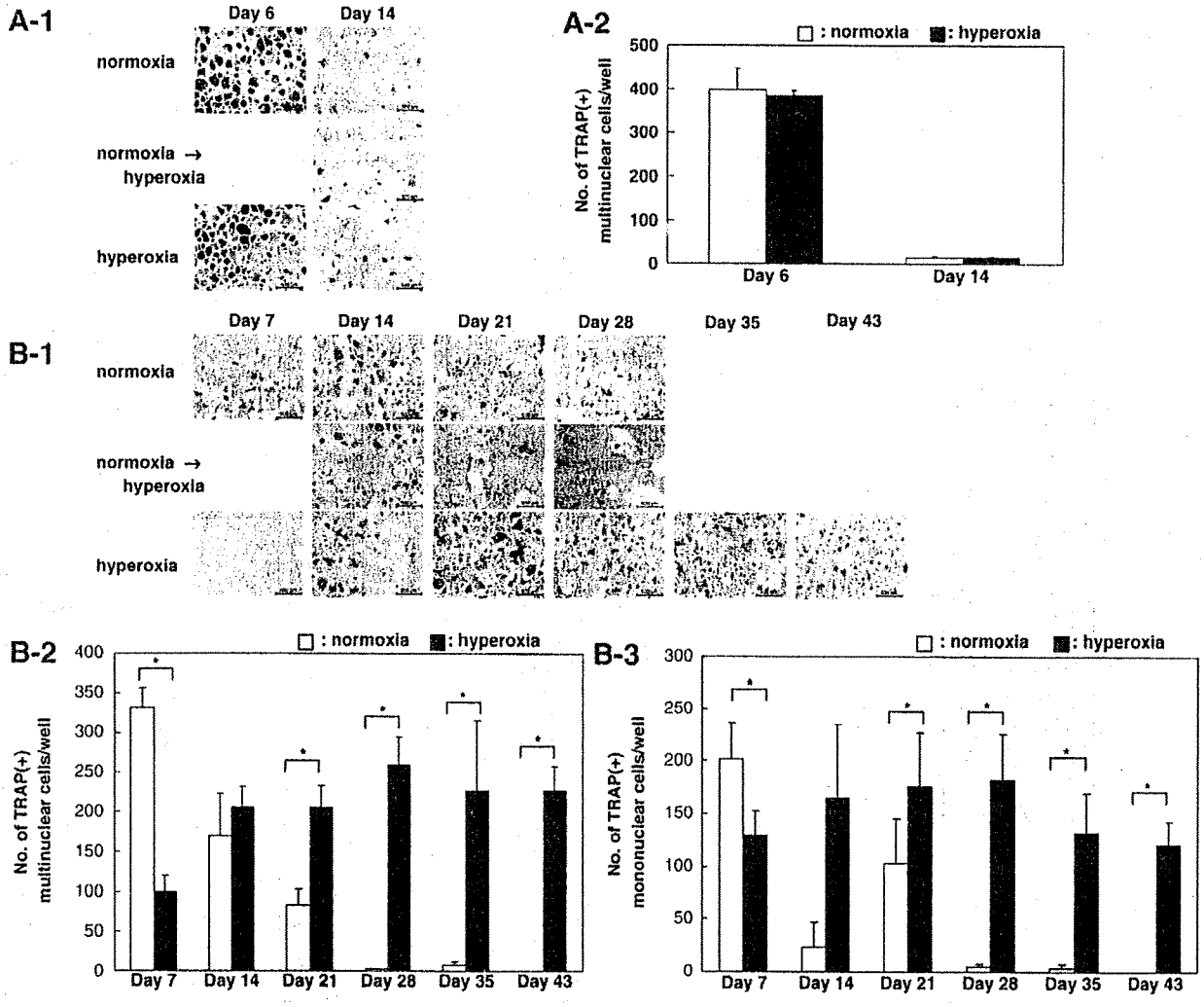

Fig. 1. Osteoclast formation from CD14+ monocytes. (A) CD14+ monocytes were cultured for 14 days with macrophage colony-stimulating factor (M-CSF: 25 ng/ml) and RANKL (40 ng/ml) under normoxic (20% O_2), normoxic to hyperoxic (N→H), or hyperoxic (40% O_2) conditions. Cultures were fixed each week and stained for tartrate-resistant acid phosphate (TRAP). Bar=500 μm (A-1). The number of TRAP-positive multinuclear cells with more than 3 nuclei was counted after 6 and 14 days of normoxia or hyperoxia (A-2). Data are shown as mean±S.D. (n=3) □, normoxia; ■, hyperoxia. (B-1) CD14+ monocytes were co-cultured with supporting cells (osteoblast-like SaOs-4/3 cells) in the presence of human parathyroid hormone (PTH: 10^{-8} M) under normoxic, normoxic to hyperoxic, or hyperoxic conditions and then fixed and stained for TRAP each week for up to 43 days. Bar=500 μm. (B-2, 3) Longer duration of osteoclast formation in cultures with supporting cells under hyperoxic conditions. (B-2) The number of TRAP-positive multinuclear cells with more than 3 nuclei in cultures with supporting cells under normoxic or hyperoxic conditions was counted each week. (B-3) The number of TRAP-positive mononuclear cells (osteoclast precursors) under normoxic or hyperoxic conditions was counted each week. *<0.001. Data are shown as mean±S.D. (n=4) □, normoxia; ■, hyperoxia.

were cultured with SaOs-4/3 cells in the presence of PTH. As shown in Fig. 1B, TRAP-positive cells formed by day 7 under normoxic conditions, but disappeared by days 14–21. With N→H culture, the newly formed CD14+ cells also disappeared by days 14–21. On other hand, TRAP-positive cells formed more slowly in hyperoxic than normoxic cultures. It took 7–14 days for CD14+ cells cocultured with SaOs-4/3 cells to be transformed into TRAP-positive cells. However, these TRAP-positive cells persisted for more than 6 weeks, a period that was three times longer than under normoxic conditions. Because an effect of hyperoxia on TRAP-positive cell formation from CD14+ cells was observed in coculture with SaOs-4/3 cells, we counted the number of TRAP-positive multinuclear cells with more than 3 nuclei and the number of TRAP-positive mononuclear cells (osteoclast precursors) in cocultures (Fig. 1B-2,3). In normoxic cultures, the number of TRAP-positive multinuclear cells began to increase on day 7, and then decreased again until the cells were rare by day 21. On the other hand, the number of TRAP-positive multinuclear cells increased after day 14 of hyperoxic culture and such cells were detected for 6 weeks (Fig. 1B-2). Transformation of TRAP-positive mononuclear cells to osteoclast precursors followed the same pattern (Fig. 1B-3).

Hyperoxia promotes M-CSF expression by SaOs-4/3 cells and c-fms expression by CD14+ cells

To investigate the mechanism underlying the above-mentioned effects of hyperoxia, we analyzed expression of the RANK (the receptor for RANKL), dendritic cell-specific transmembrane protein (DC-STAMP), c-fms (the receptor for M-CSF), Bcl2, and Bim genes on day 3 of normoxic or hyperoxic culture of CD14+ cells (Fig. 2A). RANK and DC-STAMP are important factors for osteoclastogenesis, while Bcl2 and Bim are transcription factors associated with apoptosis. There were no significant differences between normoxia and hyperoxia with regard to expression of RANK, DC-STAMP, Bcl2 and Bim (Fig. 2B-1–4), however the expression of c-fms was up-regulated under hyperoxic conditions compared with that under normoxic conditions (Fig. 2B-5). Next, we examined expression of the M-CSF, RANKL, and OPG genes by the supporting cells (osteoblast-like SaOs-4/3 cells) under normoxic or hyperoxic conditions (Fig. 3A). We found that M-CSF expression was markedly increased at day 7 and day 10 of hyperoxia (Fig. 3B-1,2). The M-CSF protein level was also increased on day 14 by Western blot analysis (Fig. 3C-1), and secretion of M-CSF into the culture medium was up-regulated after 6 days of hyperoxia according to the results of ELISA (Fig. 3C-2). RANKL expression increased in a time-dependent manner under both normoxic and hyperoxic conditions and there was no significant difference between the two levels of oxygen (Figs. 3A, B-2). OPG expression also showed no significant differences (Figs. 3A, B-3).

Inhibition of M-CSF with a neutralizing antibody abolishes hyperoxia-induced formation of TRAP-positive cells

We analyzed the influence of a neutralizing antibody directed against human M-CSF (50 ng/ml or 500 ng/ml) on cocultures of CD14+ cells and SaOs-4/3 cells under normoxic and hyperoxic conditions.

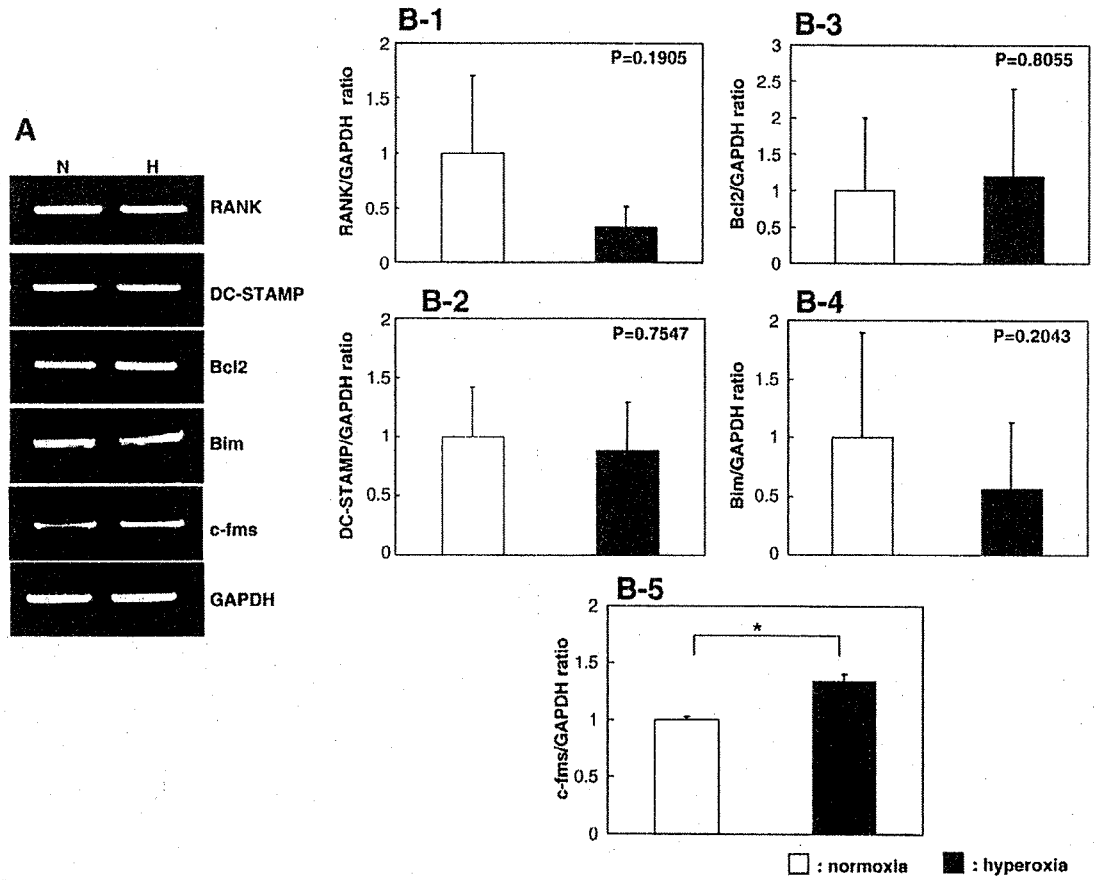

Fig. 2. Gene expression of c-fms by CD14+ monocytes increased under hyperoxia, while all other genes expression including RANK, DC-STAMP, Bcl2 and Bim did not change significantly. (A) Total RNA was extracted from CD14+ monocytes cultured under normoxic or hyperoxic conditions for 3 days, and the expression of mRNA for RANK, dendritic cell-specific transmembrane protein (DC-STAMP), Bcl2, Bim, c-fms and GAPDH was analyzed by reverse transcription polymerase chain reaction (RT-PCR). (B) Real-time PCR for RANK, DC-STAMP, Bcl2, Bim, and c-fms gene expression. Data are shown as the mean±S.D. ($n=3$) of the ratio to GAPDH for RANK (B-1), DC-STAMP (B-2), Bcl2 (B-3), Bim (B-4), and c-fms (B-5) gene expression compared with that under normoxia. Only c-fms has significantly different p value, *<0.005. □, normoxia; ■, hyperoxia.

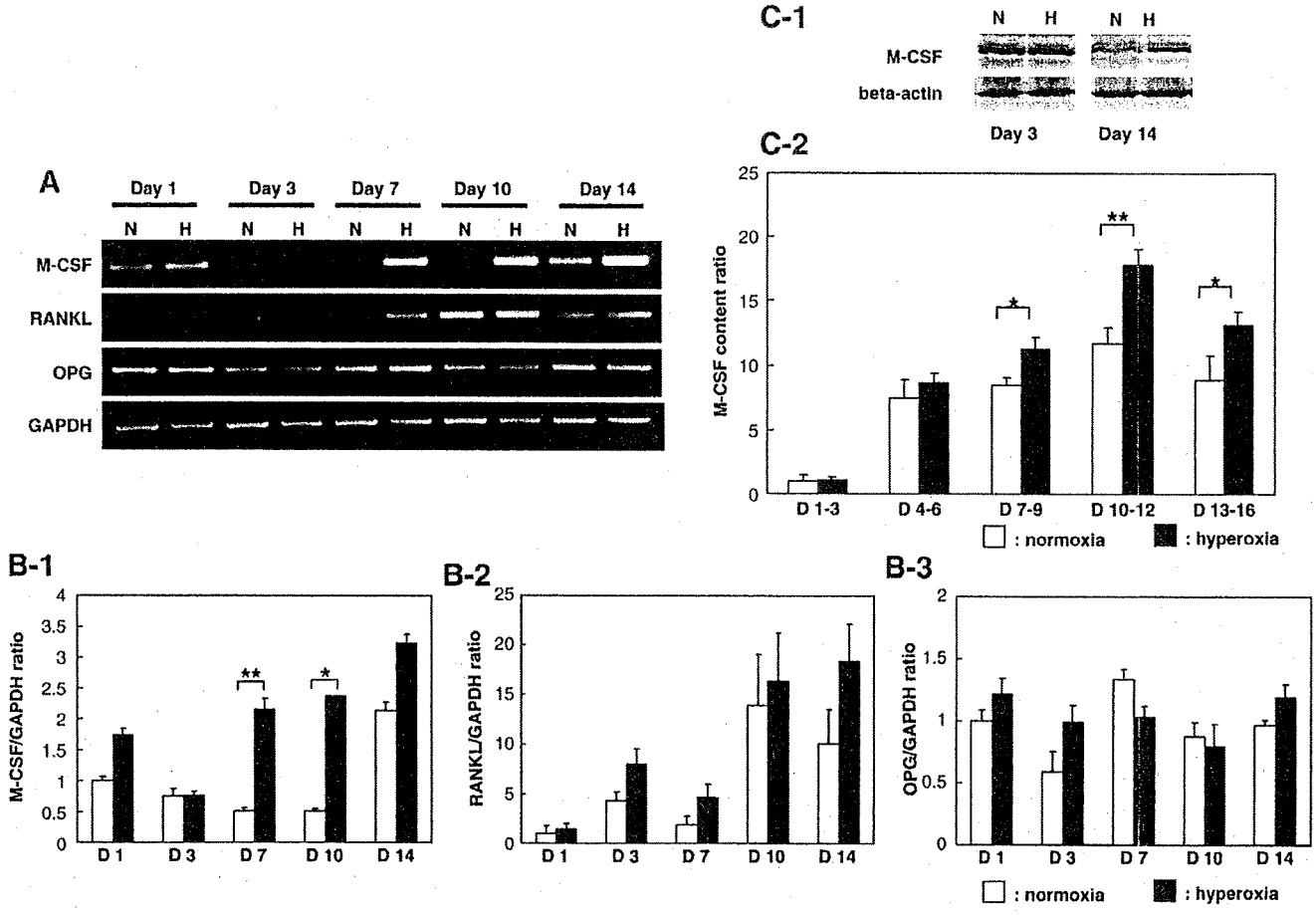

Fig. 3. Importance of M-CSF production by supporting cells for prolonged osteoclast formation under hyperoxia. SaOS-4/3 cells (5×10^6 cells/dish) were cultured for 1, 3, 7, 10, or 14 days in the presence of PTH (10^{-8} M) under normoxic or hyperoxic conditions. Total RNA was extracted from the cells, and subjected to RT-PCR to detect RANKL, OPG, and M-CSF mRNA expression. (A) Total RNA was extracted from SaOs-4/3 cells cultured under normoxic or hyperoxic conditions for 1, 3, 7, 10 or 14 days and the expression of mRNA for M-CSF, RANKL, osteoprotegrin (OPG), and GAPDH was analyzed by RT-PCR. (B) Real-time PCR for M-CSF and RANKL gene expression. Data are shown as the mean±S.D. ($n=3$) of the ratio of RANKL (B-1), M-CSF (B-2), and OPG (B-3) gene expression to GADPH compared with that under normoxic conditions on day 1. **<0.05, *<0.0005. □, normoxia; ■, hyperoxia. (C-1) SaOs-4/3 cells were cultured for 3 and 14 days under normoxic or hyperoxic conditions and lysed. The cell lysates were subjected to Western blotting with an anti-human M-CSF antibody. (C-2) Culture medium was harvested on day 3 (days 1–3), day 6 (days 4–6), day 9 (days 7–9), day 12 (days 10–12), and day 16 (days 13–16) for measurement of the M-CSF protein content by ELISA. Data are normalized by the total number of cells/well, and are shown as the mean±S.D. ($n=4$). **<0.001, *<0.01. □, normoxia; ■, hyperoxia.

After 1 week, the number of TRAP-positive multinuclear cells was decreased in a dose-dependent manner in both groups (Fig. 4A). From 2 weeks onward, the number of TRAP-positive multinuclear cells was very low under normoxic conditions, and there was no significant difference between cultures with or without M-CSF inhibition. On the other hand, the increase in the number of TRAP-positive multinuclear cells under hyperoxic conditions was partly reversed by a low dose (50 ng/ml) of anti-M-CSF antibody and was completely abolished by a high dose (500 ng/ml) at weeks 1, 2 and 3. Thus, the antibody had a dose-dependent effect.

Furthermore, this neutralizing effect in hyperoxia was decreased in case of anti-M-CSF antibody addition at weeks 2 and 3.5 when the TRAP positive cells were formed (Fig. 4B).

Increase of ROS and TRAP-positive cells at sites of bone destruction

We wanted to investigate whether hyperoxic zones exist in pathological hypervascular lesions *in vivo*, but it is too difficult to properly measure the oxygen tension of bone tissue because there are no appropriate instruments, so we measured ROS instead. We examined the distribution of vessels, ROS, and TRAP-positive multinuclear cells at sites of bone destruction in RA patients by immunohistochemistry and TRAP staining. ROS were detected with an antibody for thymidine glycol, which is one of the reactive oxygen species. It was found that vessels were abundant at the sites of bone destruction and ROS were detected in the pathological bone tissue around the vessels. In these ROS-rich areas, a large number of TRAP-positive multinuclear cells were also detected at the borders of the damaged bone (Fig. 5A).

M-CSF is associated with ROS in bone lesions

Finally, we examined the distribution of M-CSF-positive cells in the ROS-rich areas of bone destruction in RA patients. As previously described, ROS were detected at the interface of the bone lesions and M-CSF staining was also detected very strongly in the region surrounding the damaged bone (Fig. 5B-1). On the other hand, very little ROS or M-CSF was detected in OA patients (Fig. 5B-2).

Discussion

This study has provided the first evidence that a high oxygen tension promotes the survival of human osteoclast precursors via up-regulated action of M-CSF. It was previously reported that the differentiation and activity of osteoclasts were stimulated by a low oxygen tension [14,15]. We also examined the behavior of osteoclasts

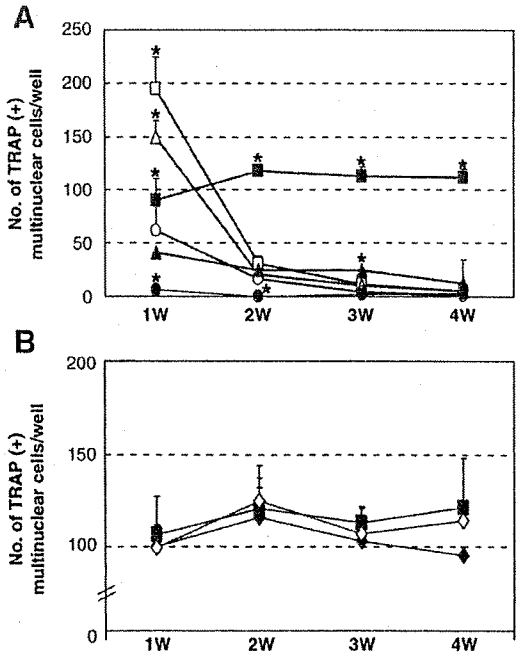

Fig. 4. M-CSF neutralizing antibody abolishes the hyperoxia-induced increase of TRAP-positive multinuclear cells with more than 3 nuclei. CD14+ monocytes were cocultured with supporting cells (SaOs-4/3 cells), and we added M-CSF neutralizing antibody against human M-CSF with increasing concentrations under normoxic or hyperoxic conditions at day 1 (final concentration; 0 ng/ml, 50 ng/ml, or 500 ng/ml) (A). The number of TRAP-positive multinuclear cells was counted each week. Data are shown as mean±S.D. ($n=3$). *<0.0001. □, 0 ng/ml neutralizing antibody under normoxia; ■, 0 ng/ml under hyperoxia; △, 50 ng/ml under normoxia; ▲, 50 ng/ml under hyperoxia; ○, 500 ng/ml under normoxia; ●, 500 ng/ml under hyperoxia. And we also added the antibody at day 14 or day 25 under hyperoxia (B) (final concentration; 500 ng/ml). ■, antibody was not added. ♦, the antibody was added at day 14 ◊, the antibody at day 25.

cultured under a low oxygen tension (5% O_2), and observed that the cells showed more rapid differentiation but shorter survival than cells cultured under a normal oxygen tension (data not shown), suggesting that osteoclastogenesis is influenced by the local oxygen tension. As mentioned earlier, both clinical and histological human data have suggested a possible positive interaction between hyperoxia and osteoclastogenesis, but it has not been confirmed. Accordingly, we investigated osteoclastogenesis using human CD14+ cells and previously reported monoculture or coculture systems [17,18,20–22]. Previously published data showed that osteoblasts or stromal cells are essentially involved in osteoclastogenesis through cell–cell interaction with osteoclast progenitors [52–54]. In monoculture system which is osteoclastogenesis from CD14+ cells with RANKL and M-CSF, almost all CD14+ cells are simultaneously differentiated into mature osteoclasts within 14 days and few of them remain after 2 weeks. On the other hand, CD14+ cells are maintained and/or differentiated depending on the local conditions given by osteoblast-like supporting cells in coculture system. Therefore, coculture system is considered to be closer to physiological *in vivo* conditions than monoculture. Referring to previous reports [23,45,46], we set the high oxygen tension at 40% O_2 and normal oxygen tension at 20% O_2.

Hyperoxia did not affect the number of osteoclasts and apoptosis, but up-regulated c-fms gene expression in monoculture

Interestingly, we could not detect any effect of a high oxygen tension on the number of osteoclasts in monoculture (Fig. 1A). When we assessed RANK, DC-STAMP, Bcl2, and Bim gene expression by CD14+ cells in monoculture, we could not detect any significant influence of hyperoxia on these genes, which are essential factors for the differentiation and apoptosis of osteoclasts. RANK is required for the differentiation of precursors to mature osteoclasts [24], while DC-STAMP plays an important role in macrophage fusion [25,26]. Bcl2 and Bim are associated with apoptosis, with Bcl2 being an inhibitor of apoptosis and Bim acting as a stimulator [27,28]. Meanwhile, when we assessed the expression of c-fms gene which is critical for osteoclastogenesis as the receptor of M-CSF, we detected up-regulated c-fms gene expression of CD14+ cells in hyperoxia. This result suggested that the CD14+ cells in hyperoxia could respond to M-CSF more sensitively.

Hyperoxia promoted continuous osteoclastogenesis for up to 43 days in coculture

On the other hand, the TRAP-positive cells were continuously recruited for three times longer period in hyperoxic coculture compared with normoxic coculture (Fig. 1B). The time course of osteoclast formation and the number of osteoclasts in coculture system often vary among donors as pointed out by previously published studies [48,49]. The variation of data in our study was relatively high and data in normoxia also varied in Figs. 1B-2 and 4A, however, the effect of hyperoxia on osteoclastogenesis was constant independent from donors. The differences in TRAP-positive cell number on days 21, 28, 35 and 43 between hyperoxia and normoxia were also statistically significant. These results in coculture system different from monoculture indicate that the supporting cells have an important role in osteoclastogenesis of CD14+ cells under hyperoxic conditions.

We also detected an influence of hyperoxia on M-CSF gene and protein expression by the supporting cells. M-CSF, RANKL, and OPG are produced by osteoblasts, and are essential factors for osteoclastogenesis. OPG acts as a decoy receptor for RANKL [29]. M-CSF gene expression was dramatically increased for at least 14 days under hyperoxic conditions (Fig. 3A), while RANKL and OPG were not significantly altered. Furthermore, gene expression of c-fms which is the receptor for M-CSF was increased in CD14+ cells (Fig. 2B-5). These findings suggest that M-CSF signaling from osteoblasts to CD14+ cells has an important role at a high oxygen tension rather than the RANKL-RANK system.

To determine whether hyperoxia affects osteoclast precursors or mature osteoclasts, we also cultured cells under normoxic conditions until mature osteoclasts formed (day 6), followed by a switch to hyperoxic conditions. Interestingly, exposure to hyperoxia after osteoclasts had developed showed no influence on TRAP staining (Figs. 1A-1, B-1), suggesting that a high oxygen tension does not act on mature osteoclasts but instead affects osteoclast precursors. These data agree with previously published data. M-CSF is essential for the survival of osteoclast precursors [16,30–35] and Woo et al [32] pointed out that M-CSF decreased the apoptosis of osteoclast precursors on a dose dependent manner by up-regulating Bcl-X_L which has an anti-apoptotic effect. All these observations indicated that hyperoxia continuously promoted M-CSF production by SaOs-4/3 cells and c-fms expression in CD14+ cells, which maintained viable osteoclast precursors for a longer period and resulted in the continuous recruitment of mature osteoclasts for 43 days in coculture.

Action of M-CSF is essential for continuous osteoclastogenesis in hyperoxic coculture

To confirm that hyperoxia-induced promotion of osteoclastogenesis was dependent on up-regulated action of M-CSF, we investigated the influence of an M-CSF neutralizing antibody on osteoclast precursor formation (Fig. 4A). TRAP-positive cells were almost abolished after 2 weeks of culture under normoxic conditions irrespective of the dose of antibody added on day 1 to the medium. On the other hand, osteoclast formation under hyperoxic conditions was decreased in a dose-dependent manner. These findings confirmed

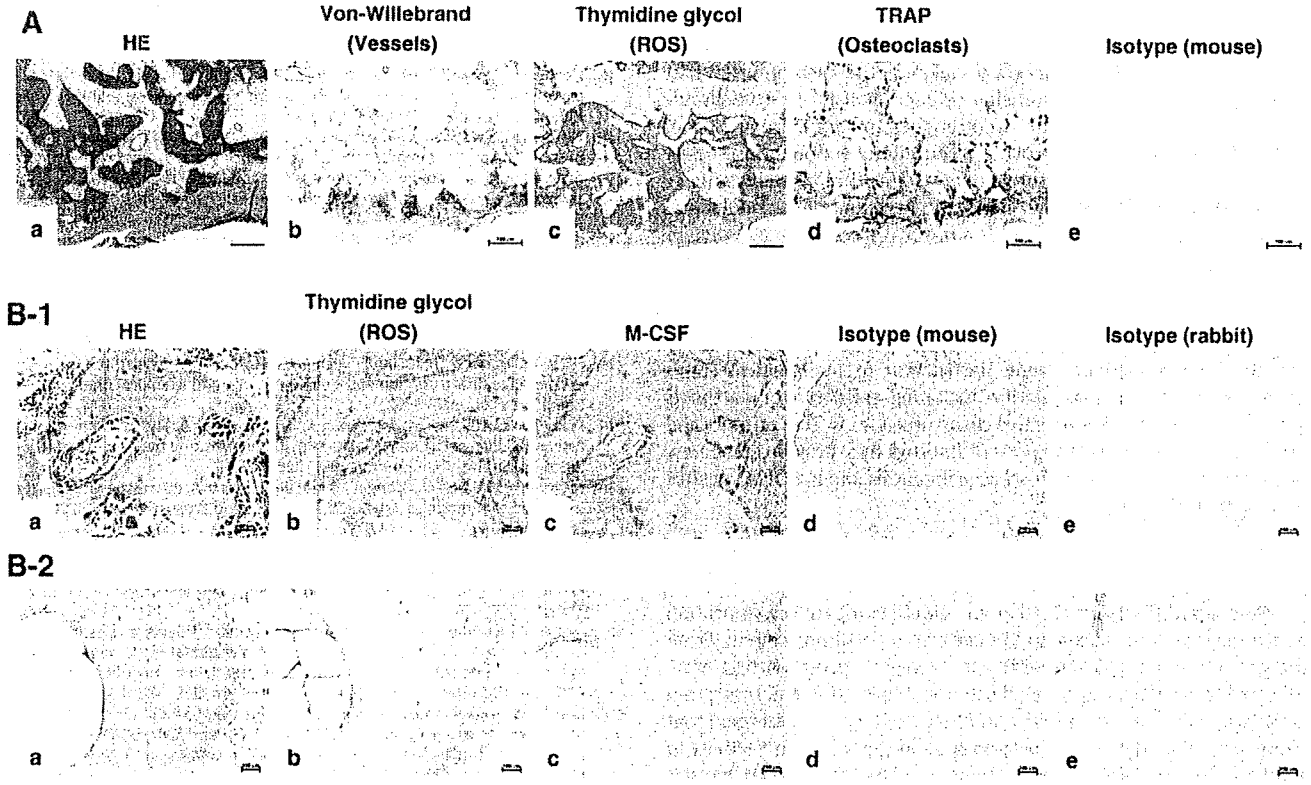

Fig. 5. (A) Localization of vessels, reactive oxygen species (ROS; thymidine glycol), and TRAP-positive cells in bone lesions. (a) H&E staining; (b) immunolocalization of von-Willebrand factor; (c) immunolocalization of ROS; (d) staining for tartrate-resistant acid phosphatase; (e) isotype control mouse IgG. Bar = 100 μm. (B) Immunolocalization of ROS and M-CSF in bone lesions of RA patients (B-1) and control tissue of OA patients (B-2). (a) H&E staining; (b) immunolocalization of ROS; (c) immunolocalization of M-CSF; (d) isotype control mouse IgG; (e) isotype control rabbit IgG. Bar = 100 μm.

that longer survival of osteoclast precursors under hyperoxic conditions was dependent on the up-regulated action of M-CSF. Interestingly, this neutralizing effect was decreased in case of the M-CSF antibody addition at 2 and 3.5 weeks after the TRAP positive cells were formed in hyperoxia (Fig. 4B). As referring to the previously published reports, M-CSF is not a critical factor for the survival of osteoclasts, while it is essential for the survival of CD14+ cells [50]. This is one of the plausible reasons why the antibody did not significantly decrease the number of TRAP positive cells after osteoclasts were already differentiated from CD14+ cells. Another possible reason is the culture-duration-dependent decrease in number of CD14+ cells because of their differentiation into osteoclasts.

However, the question arises why CD14+ cells in monoculture could not form osteoclast precursors continuously despite the addition of recombinant M-CSF and RANKL to the culture medium. TRAP-positive cells counting in monoculture showed that TRAP-positive cells appeared on day 6 and disappeared by day 14 in monoculture under both normoxia and hyperoxia (Fig. 1A-2). These data indicated that all of the CD14+ cells or osteoclast precursors had rapidly differentiated into mature osteoclasts independently of M-CSF and RANKL concentration, and few or no osteoclast precursors remain in the early days of the monoculture. This is a possible answer for the prior question. Another possible explanation is that factors other than M-CSF could be associated with the recruitment of osteoclast precursors under hyperoxia only in the coculture system. Further investigations into this issue are needed.

The association of hypervascularity, hyperoxia, and M-CSF expression

Although previous histological and clinical evaluations have shown that destructive bone lesions are accompanied by abundant neovascularization [4–10], an association among hypervascularity, a high oxygen tension, M-CSF, and osteoclasts has never been demonstrated in human tissues.

Because methods for measuring the oxygen tension in bone lesions have not been developed, we substituted the immunohistochemical detection of ROS as an indicator of the local tissue oxygen tension. Oxygen itself acts as a free radical [30], and a high oxygen tension is correlated with the production of ROS. Thus, detection of ROS implies the existence of oxidative stress [37,38], and such oxidative stress is induced in proportion to the oxygen tension [36,39,40]. We confirmed that the hyperoxic culture medium had a 2-fold higher ROS content than the normoxic medium in our vitro study (data not shown). As a result of these findings and in combination with the literature, we determined that 40% O_2 would appropriately model physiologic levels seen in RA. Therefore, we utilized ROS as a marker of a high tissue oxygen tension, and we studied the association among hypervascularity, ROS, M-CSF, and osteoclasts in bone lesions of patients with RA.

As shown in Fig. 5A, we demonstrated colocalization of hypervascularity, ROS, and TRAP-positive osteoclast-like cells on the bone surface, and furthermore, M-CSF-positive cells were increased at such abundant ROS area which is the bone destructive lesions of patients with RA (Fig. 5B-1). On the other hand, such colocalization of ROS and M-CSF was not recognized in the bone samples from OA patients (Fig. 5B-2). These histological findings indicated that hyperoxia-induced up-regulation of M-CSF production resulted in continuous osteoclast formation *in vitro*, which might reflect the actual mechanism of osteoclastic bone resorption in the hypervascular lesions of patients with RA. Enhanced production of M-CSF due to hyperoxia could provide long-term reserves of osteoclast precursors in hypervascular proliferating synovial tissue, resulting in the continuous supply of mature osteoclasts to the erosive front of affected joints in RA patients.

We previously reported that fibroblast-like synovial cells from patients with RA support the survival of osteoclast precursors via M-CSF production [16,47]. Recently, Nakano et al. also reported that M-CSF produced by RA endothelial cells is involved in osteoclastogenesis from monocytes [43]. Accordingly, enhanced production of M-CSF by hyperoxia could provide a continuing supply of osteoclast precursors that become mature osteoclasts in the affected joints of patients with RA. On the other hand, the work of Collin-Osdoby and Okada might suggest the exploration of RANKL secretion by vascular endothelial cells as a possible role [41,42]. However, our data demonstrate that RANKL expression was not altered in SaOs-4/3 cells and that RANK expression was unaltered in CD14+ cells.

Taken together, it appears that a high oxygen tension and/or oxidative stress mediates bone destruction in pathological states associated with hypervascularity, including inflammatory arthritis such as RA and rapidly destructive coxarthrosis, as well as primary and metastatic bone tumors. The present findings may provide some new insights into the processes of osteoclastogenesis and osteolysis at sites of bone pathology *in vivo*.

The limitation of this study

We realized the necessity that we should compare the resorption activity between normoxia and hyperoxia in coculture system. From the past reports associated with a low oxygen tension, Arnett et al. reported that hypoxia stimulated osteoclast formation and resorption activity in a mouse model [15], and Musylak et al. also described that hypoxia increased the size of osteoclasts and the resorption activity in a cat model [51]. These reports suggested that the oxygen tension could affect the resorption activity of osteoclasts. So, it is really interesting how hyperoxia effects on bone resorptive activity. In this study, we tried the pit formation assay in coculture system by several times, but the human coculture system is too delicate to form mature osteoclasts on dentine slices. Unfortunately we could not solve the reason and not have evaluated the resorption activity yet. So, about this problem, further studies will be needed.

In conclusion, our data suggest that a high oxygen tension dramatically prolongs osteoclast precursor formation as a result of the continuous up-regulation of M-CSF production by supporting cells and c-fms gene up-regulation in CD14+ cells. An increase of M-CSF-expressing cells and TRAP-positive cells is detected in hypervascular bone lesions along with high levels of ROS.

Acknowledgments

We would like to thank Mari Shinkawa for her excellent technical assistance, and N. Udagawa, PhD. (Matsumoto Dental University) for donating the SaOs-4/3 cells.

References

[1] Bathurst N, Sanerkin N, Watt I. Osteoclast-rich osteosarcoma. Br J Radiol 1986;59:667–73.
[2] Romas E, Gillespie MT, Martin TJ. Involvement of receptor activator of NFkappaB ligand and tumor necrosis factor-alpha in bone destruction in rheumatoid arthritis. Bone 2002;30:340–6.
[3] Yamakawa T, Sudo A, Tanaka M, Uchida A. Microvascular density of rapidly destructive arthropathy of the hip joint. J Orthop Surg (Hong Kong) 2005;13:40–5.
[4] Kindle L, Rothe L, Kriss M, Osdoby P, Collin-Osdoby P. Human microvascular endothelial cell activation by IL-1 and TNF-alpha stimulates the adhesion and transendothelial migration of circulating human CD14+ monocytes that develop with RANKL into functional osteoclasts. J Bone Miner Res 2006;21:193–206.
[5] Malemud CJ. Growth hormone, VEGF and FGF: involvement in rheumatoid arthritis. Clin Chim Acta 2007;375:10–9.
[6] Koizumi F, Matsuno H, Wakaki K, Ishii Y, Kurashige Y, Nakamura H. Synovitis in rheumatoid arthritis: scoring of characteristic histopathological features. Pathol Int 1999;49:298–304.
[7] Rooney M, Condell D, Quinlan W, Daly L, Whelan A, Feighery C, et al. Analysis of the histologic variation of synovitis in rheumatoid arthritis. Arthritis Rheum 1988;31:956–63.
[8] Matsuno H, Yudoh K, Nakazawa F, Koizumi F. Relationship between histological findings and clinical findings in rheumatoid arthritis. Pathol Int 2002;52:527–33.
[9] Hoang BH, Dyke JP, Koutcher JA, Huvos AG, Mizobuchi H, Mazza BA, et al. VEGF expression in osteosarcoma correlates with vascular permeability by dynamic MRI. Clin Orthop Relat Res 2004;426:32–8.
[10] Kajihara M, Sugawara Y, Sakayama K, Kikuchi K, Mochizuki T, Murase K. Evaluation of tumor blood flow in musculoskeletal lesions: dynamic contrast-enhanced MR imaging and its possibility when monitoring the response to preoperative chemotherapy-work in progress. Radiat Med 2007;25:94–105.
[11] Winding B, Misander H, Sveigaard C, Therkildsen B, Jakobsen M, Overgaard T, et al. Human breast cancer cells induced angiogenesis, recruitment, and activation of osteoclasts in osteolytic metastasis. J Cancer Res Clin Oncol 2000;126:631–40.
[12] Hirao M, Hashimoto J, Yamasaki N, Ando W, Tsuboi H, Myoui A, et al. Oxygen tension is an important mediator of the transformation of osteoblasts to osteocytes. J Bone Miner Metab 2007;25:266–76.
[13] Hirao M, Tamai N, Tsumaki N, Yoshikawa H, Myoui A. Oxygen tension regulates chondrocyte differentiation and function during endochondral ossification. J Biol Chem 2006;281:31079–92.
[14] Fukuoka H, Aoyama M, Miyazawa K, Asai K, Goto S. Hypoxic stress enhances osteoclast differentiation via increasing IGF2 production by non-osteoclastic cells. Biochem Biophys Res Commun 2005;328:885–94.
[15] Arnett TR, Gibbons DC, Utting JC, Orriss IR, Hoebertz A, Rosendaal M, et al. Hypoxia is a major stimulator of osteoclast formation and bone resorption. J Cell Physiol 2003;196:2–8.
[16] Tsuboi H, Udagawa N, Hashimoto J, Yoshikawa H, Takahashi N, Ochi T. Nurse-like cells from patients with rheumatoid arthritis support the survival of osteoclast precursors via macrophage colony-stimulating factor production. Arthritis Rheum 2005;52:3819–28.
[17] Matsuzaki K, Katayama K, Takahashi Y, Nakamura I, Udagawa N, Tsurukai T, et al. Human osteoclast-like cells are formed from peripheral blood mononuclear cells in a coculture with SaOS-2 cells transfected with the parathyroid hormone (PTH)/PTH-related protein receptor gene. Endocrinology 1999;140:925–32.
[18] Itoh K, Udagawa N, Matsuzaki K, Takami M, Amano H, Shinki T, et al. Importance of membrane- or matrix-associated forms of M-CSF and RANKL/ODF in osteoclastogenesis supported by SaOS-4/3 cells expressing recombinant PTH/PTHrP receptors. J Bone Miner Res 2000;15:1766–75.
[19] Arnett FC, Edworthy SM, Bloch DA, McShane DJ, Fries JF, Cooper NS, et al. The American Rheumatism Association 1987 revised criteria for the classification of rheumatoid arthritis. Arthritis Rheum 1988;31:315–24.
[20] Flanagan AM, Massey HM. Generating human osteoclasts *in vitro* from bone marrow and peripheral blood. Methods Mol Med 2003;80:113–28.
[21] Matsuzaki K, Udagawa N, Takahashi N, Yamaguchi K, Yasuda H, Shima N, et al. Osteoclast differentiation factor (ODF) induces osteoclast-like cell formation in human peripheral blood mononuclear cell cultures. Biochem Biophys Res Commun 1998;246:199–204.
[22] Kirstein B, Grabowska U, Samuelsson B, Shiroo M, Chambers TJ, Fuller K. A novel assay for analysis of the regulation of the function of human osteoclasts. J Transl Med 2006;4:45.
[23] von Zglinicki T, Saretzki G, Docke W, Lotze C. Mild hyperoxia shortens telomeres and inhibits proliferation of fibroblasts: a model for senescence? Exp Cell Res 1995;220:186–93.
[24] Teitelbaum SL. Osteoclasts: what do they do and how do they do it? Am J Pathol 2007;170:427–35.
[25] Vignery A. Macrophage fusion: the making of osteoclasts and giant cells. J Exp Med 2005;202:337–40.
[26] Kukita T, Wada N, Kukita A, Kakimoto T, Sandra F, Toh K, et al. RANKL-induced DC-STAMP is essential for osteoclastogenesis. J Exp Med 2004;200:941–6.
[27] Akiyama T, Bouillet P, Miyazaki T, Kadono Y, Chikuda H, Chung UI, et al. Regulation of osteoclast apoptosis by ubiquitination of proapoptotic BH3-only Bcl-2 family member Bim. EMBO J 2003;22:6653–64.
[28] Akiyama T, Miyazaki T, Bouillet P, Nakamura K, Strasser A, Tanaka S. In vitro and *in vivo* assays for osteoclast apoptosis. Biol Proced Online 2005;7:48–59.
[29] Nakamura M, Udagawa N, Matsuura S, Mogi M, Nakamura H, Horiuchi H, et al. Osteoprotegerin regulates bone formation through a coupling mechanism with bone resorption. Endocrinology 2003;144:5441–9.
[30] Tsurukai T, Udagawa N, Matsuzaki K, Takahashi N, Suda T. Roles of macrophage-colony stimulating factor and osteoclast differentiation factor in osteoclastogenesis. J Bone Miner Metab 2000;18:177–84.
[31] Glantschnig H, Fisher JE, Wesolowski G, Rodan GA, Reszka AA. M-CSF, TNFalpha and RANK ligand promote osteoclast survival by signaling through mTOR/S6 kinase. Cell Death Differ 2003;10:1165–77.
[32] Woo KM, Kim HM, Ko JS. Macrophage colony-stimulating factor promotes the survival of osteoclast precursors by up-regulating Bcl-X(L). Exp Mol Med 2002;34:340–6.
[33] Bouyer P, Sakai H, Itokawa T, Kawano T, Fulton CM, Boron WF, et al. Colony-stimulating factor-1 increases osteoclast intracellular pH and promotes survival via the electroneutral Na/HCO_3 cotransporter NBCn1. Endocrinology 2007;148:831–40.
[34] Okahashi N, Koide M, Jimi E, Suda T, Nishihara T. Caspases (interleukin-1beta-converting enzyme family proteases) are involved in the regulation of the survival of osteoclasts. Bone 1998;23:33–41.
[35] Tanaka S, Miyazaki T, Fukuda A, Akiyama T, Kadono Y, Wakeyama H, et al. Molecular mechanism of the life and death of the osteoclast. Ann N Y Acad Sci 2006;1068:180–6.

[36] Tuttle SW, Maity A, Oprysko PR, Kachur AV, Ayene IS, Biaglow JE, et al. Detection of reactive oxygen species via endogenous oxidative pentose phosphate cycle activity in response to oxygen concentration: implications for HIF-1alpha stability under moderate hypoxia. J Biol Chem 2007;282:36790–6.
[37] Henrotin Y, Kurz B, Aigner T. Oxygen and reactive oxygen species in cartilage degradation: friends or foes? Osteoarthr Cartil 2005;13:643–54.
[38] Correa GA, Rumpf R, Mundim TC, Franco MM, Dode MA. Oxygen tension during *in vitro* culture of bovine embryos: effect in production and expression of genes related to oxidative stress. Anim Reprod Sci 2007;104:132–42.
[39] Flandin P, Donati Y, Barazzone-Argiroffo C, Muzzin P. Hyperoxia-mediated oxidative stress increases expression of UCP3 mRNA and protein in skeletal muscle. FEBS Lett 2005;579:3411–5.
[40] Chang E, Hornick K, Fritz KI, Mishra OP, Delivoria-Papadopoulos M. Effect of hyperoxia on cortical neuronal nuclear function and programmed cell death mechanisms. Neurochem Res 2007;32:1142–9.
[41] Collin-Osdoby P, Rothe L, Anderson F, Nelson M, Maloney W, Osdoby P. Receptor activator of NF-kappa B and osteoprotegerin expression by human microvascular endothelial cells, regulation by inflammatory cytokines, and role in human osteoclastogenesis. J Biol Chem 2001;276:20659–72.
[42] Okada T, Akikusa S, Okuno H, Kodaka M. Bone marrow metastatic myeloma cells promote osteoclastogenesis through RANKL on endothelial cells. Clin Exp Metastasis 2003;20:639–46.
[43] Nakano K, Okada Y, Saito K, Tanikawa R, Sawamukai N, Sasaguri Y, et al. Rheumatoid synovial endothelial cells produce macrophage colony-stimulating factor leading to osteoclastogenesis in rheumatoid arthritis. Rheumatology (Oxford) 2007;46:597–603.
[44] Kizaka-Kondoh S, Inoue M, Harada H, Hiraoka M. Tumor hypoxia: a target for selective cancer therapy. Cancer Sci 2003;94:1021–8.
[45] Goto Y, Noda Y, Mori T, Nakano M. Increased generation of reactive oxygen species in embryos cultured in vitro. Free Radic Biol Med 1993;15:69–75.
[46] Kurosawa H, Kimura M, Noda T, Amano Y. Effect of oxygen on in vitro differentiation of mouse embryonic stem cells. J Biosci Bioeng 2006;101:26–30.
[47] Ando W, Hashimoto J, Nampei A, Tsuboi H, Tateishi K, Ono T, et al. Imatinib mesylate inhibits osteoclastogenesis and joint destruction in rats with collagen-induced arthritis (CIA). J Bone Miner Metab 2006;24:274–82.
[48] Sabokbar A, Athanasou NS. Generating human osteoclasts from peripheral blood. Methods Mol Med 2003;80:101–11.
[49] Kreja L, Liedert A, Schmidt C, Claes L, Ignatius A. Influence of receptor activator of nuclear (NF)-kappaB ligand (RANKL), macrophage-colony stimulating factor (M-CSF) and fetal calf serum on human osteoclast formation and activity. J Mol Histol 2007;38:341–5.
[50] Udagawa N, Takahashi N, Jimi E, Matsuzaki K, Tsurukai T, Itoh K, et al. Osteoblasts/stromal cells stimulate osteoclast activation through expression of osteoclast differentiation factor/RANKL but not macrophage colony-stimulating factor. Bone 1999;25:517–23.
[51] Muzylak M, Price JS, Horton A. Hypoxia induces giant osteoclasts formation and extensive bone resorption in the cat. Calcif Tissue Int 2006;79:301–9.
[52] Yasuda H, Shima N, Nakagawa N, Yamaguchi K, Kinosaki M, Goto M, et al. A novel molecular mechanism modulating osteoclast differentiation and function. Bone 1999;25:109–13.
[53] Suda T, Kobayashi K, Jimi E, Udagawa N, Takahashi N. The molecular basis of osteoclast differentiation and activation. Novartis Found Symp 2001;232:235–47.
[54] Katagiri T, Takahashi N. Regulatory mechanism of osteoblast and osteoclast differentiation. Oral Dis 2002;8:147–59.

DNA Research 13, 169–183 (2006) doi:10.1093/dnares/dsl006

Isolation and Expression Profiling of Genes Upregulated in Bone Marrow-Derived Mononuclear Cells of Rheumatoid Arthritis Patients

Nobuo Nakamura,[1,†] Yasunori Shimaoka,[2,†] Takahiro Tougan,[3] Hiroaki Onda,[3,4] Daisuke Okuzaki,[3] Hanjun Zhao,[3] Azumi Fujimori,[3] Norikazu Yabuta,[3] Ippei Nagamori,[3] Akie Tanigawa,[4] Jun Sato,[3] Takenori Oda,[5] Kenji Hayashida,[6] Ryuji Suzuki,[7] Masao Yukioka,[2] Hiroshi Nojima,[3,4,*] and Takahiro Ochi[7]

Center of Arthroplasty, Kyowakai Hospital, Suita, Japan[1], Yukioka Hospital, Osaka, Japan[2], Department of Molecular Genetics, Research Institute for Microbial Diseases, Osaka University, 3-1 Yamadaoka, Suita, Osaka 562-0031, Japan[3], Innovation Plaza Osaka, Izumi, Japan[4], Department of Rheumatology, NHO Osaka-Minami Medical Center, Kawachinagano, Japan[5], Hoshigaoka Kosei-Nenkin Hospital, Hirakata, Japan[6] and Clinical Research Center for Allergy and Rheumatology, National Sagamihara Hospital, 18-1 Sakura-dai, Sagamihara, Kanagawa 228-8522, Japan[7]

(Received 25 July 2006; revised 21 August 2006)

Abstract

We have comprehensively identified the genes whose expressions are augmented in bone marrow-derived mononuclear cells (BMMC) from patients with Rheumatoid Arthritis (RA) as compared with BMMCs from Osteoarthritis (OA) patients, and named them *AURA* after *au*gmented in *RA*. Both stepwise subtractive hybridization and microarray analyses were used to identify *AURA* genes, which were confirmed by northern blot analysis and/or reverse transcription polymerase chain reaction (RT–PCR). We also assessed their expression levels in individual patients by quantitative real-time RT–PCR. Of 103 *AURA* genes we have identified, the mRNA levels of the following 10 genes, which are somehow related to immune responses, were increased in many of the RA patients: *AREG* (=*AURA9*), FK506-binding protein 5 (FKBP5 = *AURA45*), C-type lectin superfamily member 9 (*CLECSF9* = *AURA24*), tyrosylprotein sulfotransferase 1 (*TPST1* = *AURA52*), lymphocyte G0/G1 switch gene (*G0S2* = *AURA8*), chemokine receptor 4 (CXCR4 = *AURA86*), nuclear factor-kappa B (NF-κB = *AURA25*) and two genes of unknown function (FLJ11106 = *AURA1*, BC022398 = *AURA2* and XM_058513 = *AURA17*). Since *AREG* was most significantly increased in many of the RA patients, we subjected it to further analysis and found that AREG-epidermal growth factor receptor signaling is highly activated in synovial cells isolated from RA patients, but not in OA synoviocytes. We propose that the expression profiling of these *AURA* genes may improve our understanding of the pathogenesis of RA.

Key words: stepwise subtraction; microarray; RA; OA; amphiregulin; synoviolin

1. Introduction

Rheumatoid arthritis (RA) is a systemic autoimmune disease characterized by arthritis that predominantly results in chronic inflammation of systemic joints associated with the overgrowth of synovial cells. This induces progressive cartilage and bone destruction in the joint and subsequent disability. Since RA pathogenesis is likely to involve genetic elements, a number of groups have subjected samples from healthy and affected individuals to DNA microarray analyses for a broad-scale comparison. These studies have provided

Communicated by Mitsuo Oshimura

* To whom correspondence should be addressed. Tel. +81-6-6875-3980, Fax. +81-6-6875-5192, E-mail: snj-0212@biken.osaka-u.ac.jp

† These authors contributed equally to this work.

© The Author 2006. Kazusa DNA Research Institute.

The online version of this article has been published under an open access model. Users are entitled to use, reproduce, disseminate, or display the open access version of this article for non-commercial purposes provided that: the original authorship is properly and fully attributed; the Journal and Oxford University Press are attributed as the original place of publication with the correct citation details given; if an article is subsequently reproduced or disseminated not in its entirety but only in part or as a derivative work this must be clearly indicated. For commercial re-use, please contact journals.permissions@oxfordjournals.org

significant insights into RA pathogenesis.[1,2] The first samples tested were synovial specimens,[3–8] and peripheral blood mononuclear cells (PBMC),[9] from RA and osteoarthritis (OA) patients, and cluster analysis of the resulting microarray gene-expression data revealed some candidate genes that may play a specific role in RA pathogenesis.

In other studies searching for key factors in RA pathogenesis, immunoscreening by using an antirheumatoid synovial cell antibody identified synoviolin/Hrd1 to be a highly expressed enzyme (E3 ubiquitin ligase) in the rheumatoid synovium.[10] Synoviolin appears to be a pathogenic factor for RA because mice overexpressing this enzyme developed spontaneous arthropathy, while heterozygous knockdown results in increased synovial cell apoptosis and resistance to collagen-induced arthritis.[11] It was proposed that the excess elimination of unfolded proteins due to synoviolin overexpression triggers synovial cell overgrowth.[12] Thus, synoviolin may play a pivotal role in the pathogenesis of arthropathy due to its functions in the quality control of proteins through the endoplasmic reticulum (ER)-associated degradation (ERAD) system; its elevated expression may therefore have an anti-apoptotic effect that causes synovial hyperplasia.

Bone marrow-derived mononuclear cells (BMMC) are another target for analyses aiming to identify the key genes that participate in RA pathogenesis because accumulating evidence suggests that BMMC cell abnormalities may contribute to the pathogenesis of RA and experimental arthritis models.[13–17] Moreover, RA patients suffer from defective central and peripheral B-cell tolerance checkpoints,[18] the first of which occurs in the bone marrow between the early immature and immature B-cell stages (the second counter selection step of autoantibody-expressing B cells takes place in the periphery, when the new emigrant becomes a mature naive B cell).[18,19] In addition, inflammatory changes similar to those found in RA synovium seem to occur in the subchondral bone marrow of the involved RA joint,[20] and synovial inflammatory tissue can reach the adjacent bone marrow by fully breaking the cortical barrier.[21] Thus, BMMC cells are an interesting subject for studies seeking to identify specific genes involved in RA pathogenesis.

To identify the genes whose expressions are dramatically induced or reduced in the pooled BMMC mRNAs of 50 RA patients as compared with 50 OA patients, we here subjected these pooled mRNAs to stepwise subtraction, which is a unique technique that we have developed previously.[22] This method permitted the comprehensive identification of those genes that are specifically up- or down-regulated during RA pathogenesis. In addition, we also used microarray analysis, since DNA microarray analyses on the BMMC of RA patients have not been described previously. As a control, we also subjected the BMMC RNA from OA patients to stepwise subtraction and microarray analysis to identify the genes that are specifically involved in OA pathogenesis. These analyses together resulted in the isolation of 103 RA-upregulated genes, of which amphiregulin (AREG) was revealed by quantitative real-time RT–PCR (QRT–PCR) to be the most conspicuously induced gene in RA patients. Interestingly, we also show here that AREG operates upstream of synoviolin in isolated synovial cells through an epidermal growth factor receptor (EFGR) signaling pathway. We discuss how AREG upregulation could contribute to RA pathogenesis.

2. Patients, Materials and Methods

2.1. Human subjects and ethical considerations

All RA patients satisfied the 1987 revised diagnostic criteria of the American College of Rheumatology (ACR: formerly the American Rheumatism Association).[23] All OA patients fulfilled the ACR criteria for hip or knee OA.[24] The RA and OA patient groups were largely matched in terms of their average age and sex (Supplementary Figure S1A and B). This study was reviewed and approved by the Internal Review Board of the Research Institute for Microbial Diseases, Osaka University. Accordingly, a written informed consent was obtained from each participant before obtaining human tissues.

2.2. Cell proliferation assay

The synovial cells from each patient were seeded onto uncoated 35 mm tissue culture plates at 1×10^5 cells/well and cultured in 5% FBS/DMEM. After 12 h, the cells were incubated in fresh 5% FBS/DMEM with (100 ng/ml) or without AREG (Sigma-Aldrich, A 7080). Four photos were taken from fixed areas in four quadrants near the central area of each plate at the 0, 1, 3 and 4 day time points. The cells at each time point were counted from these four photos and expressed as mean ± standard error (SE).

2.3. Statistical analysis

Significant differences were determined using the Spearman's rank correlation (Supplemenatry Figure S4) or the Mann–Whitney *U*-test (Figs 2, 4 and Supplementary Figure S3). The data are expressed as means ± SE. $P < 0.05$ or $P < 0.01$ was considered to be statistically significant.

3. RESULTS

3.1. Identification of RA- or OA-specific genes by stepwise subtraction and DNA microarray analysis

To isolate the putative RA-specific genes that are upregulated in BMMC of RA patients relative to those

Figure 1. Northern blot or RT–PCR analysis of individual *AURA* cDNA clones to compare the expression levels of the genes in the BMMC of 50 RA patients and 50 OA patients (see Table 1 for their gene names). A northern blot or RT–PCR for *GAPDH* is also shown as a loading control. Left row: expression levels as detected by RT–PCR or northern blot analysis (denoted as n above each picture). Right row: confirmation of the expression level of each gene as determined by RT–PCR. The annealing temperature and amplification cycles for RT–PCR were always 50°C and 40 cycles, respectively, with the exception of the reactions denoted by a (50°C and 35 cycles, respectively), b (50°C and 30 cycles, respectively), c (55°C and 35 cycles, respectively), d (55°C and 40 cycles, respectively), and e (60°C and 40 cycles, respectively).

that are upregulated in OA patients, we first used our stepwise subtractive hybridization method. Briefly, we prepared a cDNA library from the pooled mRNA from the BMMC of 50 RA patients (Supplementary Figure S1A) by the linker-primer method using a pAP3neo vector.[25] Stepwise subtractive hybridization was then performed with the biotinylated pooled mRNA from the BMMC of 50 OA patients (Supplementary Figure S1A) to select candidate genes that may show upregulation in RA BMMC only as described previously.[22] To examine if the candidate genes are actually upregulated in RA but not OA BMMC, we performed northern blot analysis and/or RT–PCR using the pooled mRNA from the BMMC of 50 RA and 50 OA patients (Fig. 1). To reduce

the possibility of missing important RA-specific pathogenic genes by this method, we also performed a genome-wide complementary DNA microarray analysis using the Agilent Hu44K array with the same pooled RNA samples obtained from the BMMC of RA and OA patients that were described above. When we tested top 70 genes from the microarray list of RA-upregulated genes by northern blot analysis and/or RT–PCR as described above, we found that only 20 genes really displayed RA-upregulated expressions. Thus, we identified 103 RA-upregulated genes (Fig. 1) and named them *AURA* (*au*gmented in ***RA***). As shown in Table 1, 15 *AURA* genes (*AURA1*~*AURA7* and *AURA10*~*AURA17*) are uncharacterized novel genes.

We also performed similar experiments to obtain candidate OA-upregulated genes by generating a cDNA library from the pooled mRNA from the BMMC of 50 OA patients (Supplementary Figure S1A) and then using biotinylated pooled mRNA from the BMMC of 50 RA patients for subtraction (Supplementary Figure S1A). DNA microarray analysis also yielded a number of candidate OA-specific genes, as described above. However, when we checked whether these candidate genes are truly specifically up-regulated in OA BMMCs by northern blot analysis and/or RT–PCR, we could confirm this for only two genes (Supplementary Figure S2). These two OA-upregulated genes encode nuclear receptor coactivator 1 and a hypothetical protein (FLJ20581). This result suggests that the gain of function due to the enhanced expression of the RA-upregulated candidate genes is important in the pathogenesis of RA. Thus, we subsequently concentrated our study on the RA-upregulated genes.

3.2. *Expression profiles of RA-upregulated genes in individual RA or OA patients*

To determine whether the upregulation of the 103 RA-specific candidate genes is widespread in many RA patients or occurs in only a few patients, we performed QRT–PCR using individually prepared RNA samples from the BMMC or PBMC of RA patients. Of the 103 candidate genes, 5 genes whose functions are unknown and 12 genes that may be related to growth regulation or immune response were analyzed by QRT–PCR. OA patients were also examined as negative controls. In every QRT–PCR, a standard RNA from the PBMC of a healthy volunteer (male, age 52) was used (denoted as normal with a relative intensity of 1.0). This allowed us to compare the expression profiles of the genes tested in this study. In addition, since we used this control, we could also compare the expression profiles of the genes in this study with those of other genes tested in our previous reports on other autoimmune diseases.[26]

Of the 17 tested *AURA* genes (denoted x in Table 1), AREG (*AURA9*) was the most conspicuously upregulated in the BMMC of many of the RA patients, while in contrast OA BMMCs invariably expressed this gene at very low levels (Fig. 2A). Similarly, the PBMC of many RA patients strongly expressed AREG, while only very low expression was detected in the PBMC of the OA patients (Fig. 2A). AREG is one of the EGF-like growth factors that stimulate cell growth by activating the EGF receptor (EGFR) signaling of the target cells in an autocrine/juxtacrine fashion.[27]

AURA1 was the next most conspicuously upregulated gene in the BMMC of many RA patients, while the BMMC of all OA patients showed only very low expression of this gene (Fig. 2B). However, unlike *AREG*, the PBMC of RA patients showed negligible enhancement in the expression of *AURA1*. *AURA1* encodes an uncharacterized protein containing a thioesterase domain (Fig. 2B inset) that may cleave thioester bonds of an unknown target.

The gene encoding FK506 (tacrolimus)-binding protein 5 (FKBP5 = *AURA45*) also showed enhanced expression in nearly half of the RA patient BMMC samples, while no such increase was observed in the OA patient BMMC samples or in the PBMC of the RA patients (Fig. 2C). FKBP5 is a cellular receptor for FK506 and has an immunosuppressive effect on activated T cells because it inhibits the protein phosphatase calcineurin.[28]

Nearly half of the RA patient BMMC samples showed 5- to 50-fold greater expression of *CLECSF9* (=*AURA24*), *TPST1* (=*AURA52*) and *AURA2* than the normal control PBMC sample (Fig. 2D–F). No such increase was observed in the BMMC of OA patients or in the PBMC of the RA patients. *CLECSF9* encodes a macrophage-inducible C-type lectin (Mincle) that harbors a calcium-dependent carbohydrate-recognition domain. *TPST1* is one of the two Golgi tyrosylprotein sulfotransferases (*TPST1* and *TPST2*) that mediate the post-translational modification tyrosine O-sulfation.

G0S2 (=*AURA8*), chemokine receptor 4 (CXCR4 = *AURA86*), nuclear factor-kappa B (NF-κB = *AURA25*) and *AURA17* showed augmented expression in both the BMMC and PBMC of some of the RA patients when compared to the expression in the BMMC and PBMC of the OA patients, although the differences between the RA and OA samples are not as significant as for the previously discussed genes (Supplementary Figure S3A–D). G0S2 is one of the G0/G1 switch (G0S) genes that are differentially expressed in lymphocytes during their lectin-induced switch from the G0 to the G1 phases of the cell cycle.[29] CXCR4, the receptor for a chemokine called stromal cell-derived factor-1 (SDF-1/CXCL12), is important in the migration, homing and survival of hematopoietic stem cells. SDF-1, which is secreted by ischemic myocardium, is involved in the homeostatic and inflammatory traffic of leukocytes, and is highly expressed in the synovial tissues of RA patients.[30] NF-κB

Table 1. List of *AURA* genes

AURA no.	Accession no.	Sequence description	SS/DM	QRT–PCR
AURA1	AK001968	Unknown cDNA (FLJ11106)	b	r
AURA2	BC022398	Unknown cDNA	b	r
AURA3	BC031341	Unknown cDNA (hypothetical protein MGC45871)		
AURA4	NM_052862.2	Unknown cDNA (hypothetical protein MGC21854)		
AURA5	AK097275.1	Unknown cDNA (FLJ39956) L-PLASTIN-like		
AURA6	BC019355	Unknown cDNA (ring finger protein 149: IMAGE:3956746)		
AURA7	AF078845.1	Unknown cDNA (16.7Kd protein)		
AURA8	M69199	Putative lymphocyte G0/G1 switch gene (G0S2)=Aile1	b	r
AURA9	AH002608	Amphiregulin	b	r
AURA10	AK026118	Unknown cDNA (Ch20-ORF43)		r
AURA11	AK094006	Unknown cDNA		
AURA12	AK095896.1	Unknown cDNA (FLJ38577)		
AURA13	BC014435	Unknown cDNA (IMAGE:4855747)		r
AURA14	ZF161365	Unknown cDNA (HSPC102)	m	
AURA15	FLJ23431	Unknown cDNA (FLJ23431) MHC class I -like		
AURA16	BC066334	Unknown cDNA (FLJ37760)		
AURA17	XM_058513	Unknown cDNA (DKFZp434H2111)	m	r
AURA18	BC016660	Heat shock 70 kDa protein 8		
AURA19	BC022347	Lactotransferrin		
AURA20	NM_001800.2	Cyclin-dependent kinase inhibitor 2D (p19) (CDKN2D)		
AURA21	X55668.1	Proteinase 3		
AURA22	BC013946	Kruppel-like factor 13		
AURA23	BC022463	Dual specificity phosphatase 1 (DUSP1)		r
AURA24	AY358499	C-type lectin, superfamily member 9 (CLECSF9)	b	r
AURA25	AY033600	NF-kB alpha	b	r
AURA26	AF194172	Androgen-regulated protein 6 (AIG6)	m	
AURA27	NM_021810	Cadherin-like 26 (CDH26)		
AURA28	X52053.1	HP-1 (corticostatin/defensin family)		r
AURA29	BC018857.2	Translation elongation factor 1 gamma		
AURA30	BC053585.1	Colony stimulating factor 3 receptor (granulocyte)		
AURA31	AY124010	Interleukin 1 receptor, type II (IL1R2)	m	
AURA32	BC020635	Ficolin 1 (FCN1: collagen/fibrinogen domain-containing)		
AURA33	BC106068	Microtubule-associated protein, RP/EB family, member 1		
AURA34	AF443591	Death effector domain-containing DNA binding protein2		
AURA35	BC032491	Ubiquitin-conjugating enzyme E2L 6 (UBE2L6)		
AURA36	BC004967	Ubiquitin associated domain containing 1 (UBADC1)		
AURA37	NM_006313.1	Ubiquitin specific protease 15 (USP15)		
AURA38	BC011358	ADP-ribosylation factor 1		
AURA39	AY366510.1	Pre-mRNA 3'end processing factor FIP1		
AURA40	NM_175039.1	Sialyltransferase 7D (SIAT7D). transcript variant 2		
AURA41	BC030230.2	Aminolevulinate, delta- synthase 2		
AURA42	NM_014390.1	Staphylococcal nuclease domain containing 1 (SND1)		
AURA43	NM_015999.2	Adiponectin receptor 1 (ADIPOR1)		
AURA44	BC033877.1	Finkel-Biskis-Reilly murine sarcoma virus (FBR-MuSV)		r
AURA45	NM_004117	FK506 binding protein 5 (FKBP5)	b	r
AURA46	NM_000211.1	Integrin beta 2 (antigen CD18 (p95)		
AURA47	BC015641.2	Enolase 1 (alpha)		

Table 1. continued.

AURA no.	Accession no.	Sequence description	SS/DM	QRT-PCR
AURA48	BC028299.1	Non-POU domain containing, octamer-binding.		
AURA49	BC000734.2	Eukaryotic translation initiation factor 3, subunit 6 48 kDa		
AURA50	NM_012198.2	Grancalcin, EF-hand calcium binding protein (GCA)		
AURA51	BC026690.2	CD97 antigen, transcript variant 2,		
AURA52	CR542060	Tyrosylprotein sulfotransferase 1 (TPST1)	m	r
AURA53	NM_005875.1	Translation factor sui1 homolog (GC20)		
AURA54	NM_004048.2	Beta-2-microglobulin (B2M)		
AURA55	BC017934	NudC domain containing 2 (NUDCD2)		
AURA56	NM_000569	Fc fragment of IgG, low affinity IIIa, receptor for (CD16)	b	
AURA57	BC018649.2	Polymerase (RNA) II (DNA directed)		
AURA58	BC013293	Synuclein, alpha (a molecular chaperone)		
AURA59	NM_033405.2	PRIC285		
AURA60	J02694.1	Myeloperoxidase		
AURA61	BC020219	Zinc finger protein 143 (clone pHZ-1)	m	
AURA62	BC071590	Nijmegen breakage syndrome 1 (nibrin)		
AURA63	BC003186	DNA replication complex GINS protein PSF2		r
AURA64	NM_006060	Zinc finger protein, subfamily 1A, 1 (ZNFN1A1)		
AURA65	BC015859	T-cell activation GTPase activating protein		
AURA66	Z50749	Sds22 (protein phosphatase regulatory subunit)-like		r
AURA67	AF411850	C-type lectin-like receptor CLEC-6	m	
AURA68	BC064831	HMT1 hnRNP methyltransferase-like 3		
AURA69	BC022797	Mof4 family associated protein 1		
AURA70	BC032437	Heterogeneous nuclear ribonucleoprotein A3		
AURA71	M87790	Anti-hepatitis A immunoglobulin lambda chain variable region		
AURA72	K01763	Haptoglobin alpha(1S)-beta precursor		
AURA73	BC016800	Aldolase A, fructose-bisphosphate, transcript variant		
AURA74	BC001391	Actin-like 6A, transcript variant 1		
AURA75	NM_003512.3	H2 histone, family 2AC (H2AC)		
AURA76	BC017558	H3 histone, family 3B (H3.3B)		
AURA77	BC032748	Myosin regulatory light chain MRCL3		
AURA78	S60099	APPH = amyloid precursor protein homolog		
AURA79	BC067100	Fas (TNFRSF6) associated factor 1		
AURA80	NM_000896	Cytochrome P450, family 4, subfamily F (CYP4F3)	b	
AURA81	BC010577	Granulin (an association partner of cyclin T1)		
AURA82	AF054186	p18		
AURA83	BC028626	Trinucleotide repeat containing 6B		
AURA84	L43631	Scaffold attachment factor B (SAF-B)		
AURA85	M11124	MHC HLA DQ alpha-chain mRNA from DRw9 cell line		
AURA86	AF025375	Chemokine (C-X-C motif) receptor 4 (CXCR4)	b	r
AURA87	BC000163	Vimentin (VIM)		
AURA88	BC071860	Lactate dehydrogenase B (LDHB)		
AURA89	BC100032	Ribosomal protein S13 (RPS13)		
AURA90	BC011852	Glutamine synthetase (GLUL)		
AURA91	NM_000045	Arginase, liver (ARG1)		
AURA92	BC006510	Cyclin B1		
AURA93	BC007063	Peroxiredoxin 1		
AURA94	NM_005746	Pre-B-cell colony enhancing factor 1 (PBEF1)	m	

Table 1. continued.

AURA no.	Accession no.	Sequence description	SS/DM	QRT–PCR
AURA95	BC018711	RNA-binding region (RNP1. RRM) containing 1		
AURA96	NM_001126	Adenylosuccinate synthase (ADSS)		
AURA97	BC008929	rab2 mRNA. YPT1-related and member of ras family		
AURA98	NM_004226	Serine/threonine kinase 17b (apoptosis-inducing) (STK17B)	m	
AURA99	BC096336	Insulin-degrading enzyme		
AURA100	AF501883	G protein Beta polypeptide 2 (GNB2)		
AURA101	BC007237	Myeloid/lymphoid or mixed-lineage leukemia		
AURA102	BC034149.1	Ribosomal protein S3		
AURA103	NM_020980	Aquaporin 9 (AQP9)	m	

Of 103 *AURA* genes, 83, 10 or 10 genes were identified by stepwise subtraction (SS) alone (no mark), by DNA microarray (DM) alone (denoted by m) or by both techniques (denoted by b), respectively. The *AURA* genes that were subjected to QRT–PCR analysis are denoted by r.
PRIC285: peroxisomal proliferator-activated receptor A interacting complex 285.

is a transcription factor that resides in the cytoplasm of every cell and translocates to the nucleus when activated by a wide variety of agents, including cytokines.[31] *AURA17* is an uncharacterized novel gene that encodes a large protein with 8 leucine rich repeats, Mitochondrial Rho (Miro) motif and protein tyrosine kinase domain (Supplementary Figure S3D inset).

We also tested seven other genes in RA and OA BMMC and PBMC samples by QRT–PCR, but none showed a widespread and conspicuous increase in expression in the RA BMMC samples (data not shown). Consequently, these genes appear to play a less significant role in RA pathogenesis. Since these experiments and those described above consumed almost all BMMC and PBMC samples from the RA and OA patients, the remaining *AURA* genes will have to be tested in the future with another RA patient set.

3.3. *Expression pattern of AURA genes in PBMC*

To determine whether the *AURA* genes are expressed in particular human blood cells, we performed RT–PCR on multiple tissue cDNA panels (MTC) from Clontech (Palo Alto, CA). As shown in Fig. 3, RT–PCR detected *AREG* mRNA in both monocytes (lane 4) and T and B cells (lanes 2–4), in particular in activated $CD4^+$ T cells (lane 8). *AURA1* is detected predominantly in resting $CD4^+$ (T helper/inducer; lane 3) and activated $CD4^+$ T (lane 8) cells. *CLECSF9* is expressed in most cell types except for activated $CD19^+$ T cells (lane 6), while *G0S2* is found primarily in monocytes (lanes a and 4). *FKBP5*, *TPST1*, *CXCR4*, *AURA2* and *NFκB* are ubiquitously expressed in most cell types. Thus, the analysis of the functions these *AURA* genes, apart from *AURA1* and *G0S2*, play in specific blood cells will not be easy because they are already expressed in normal blood. However, the function of *AURA1* can be studied by using $CD4^+$ T cells of RA and OA patients. In this study, however, we could not perform this analysis because of the low amounts of BMMC that we could obtain from the RA patients.

3.4. *AREG stimulates the growth of synovial cells*

Since AREG appears to be the most conspicuously unpregulated gene in many RA patients, we subjected it to further analysis. We first examined its ability to stimulate the growth of isolated synovial cells because AREG is one of the ligands of EGFR and is known to induce cell growth. Thus, we isolated synovial cells from synovial tissues that were obtained from five RA and three OA patients during joint reconstructive surgery. In the absence of AREG in the culture medium, the synovial cells from both the RA and OA patients grew at a similar rate (Fig. 4A and B). However, when AREG was present, the synovial cells from RA patients appeared to grow slightly faster than the synovial cells from OA patients, which is statistically significant ($P < 0.05$) (Fig. 4A).

To examine if this phenomenon is reflected in the signal transduction machinery of synovial cells, we investigated the activation of the EGFR signaling pathway in the AREG-treated and untreated RA synoviocytes. We first examined the phosphorylation of the extracellular signal-regulated kinases (ERK1/2) at Thr202 and Tyr204 by western blot analysis. ERK1/2 phosphorylation indicates the activation of the EGFR signaling pathway.[32] As shown in Fig. 5A, the phosphorylated ERK1/2 bands in the RA synoviocytes showed an increase in intensity when the cells had been treated with AREG; this effect peaked 8–12 h after AREG treatment but continued for 2–3 days. In contrast, the ERK1/2 protein levels remained largely unaffected by AREG treatment.

To compare the activation of EGFR signaling between RA and OA patients, we examined the activation of the EGFR signaling pathway in the synoviocytes from the five RA and three OA patients (Fig. 5B). We thus assessed the phosphorylated ERK1/2 expression levels by western blot analysis and expressed the results quantitatively by measuring the intensity of the lower phosphorylated band by densitometry and comparing it with the ERK1/2 band intensity (Fig. 5C). We found that the synoviocytes from the RA and OA patients expressed equivalent levels of EGFR and ERK1/2 proteins, regardless of AREG treatment. In contrast,

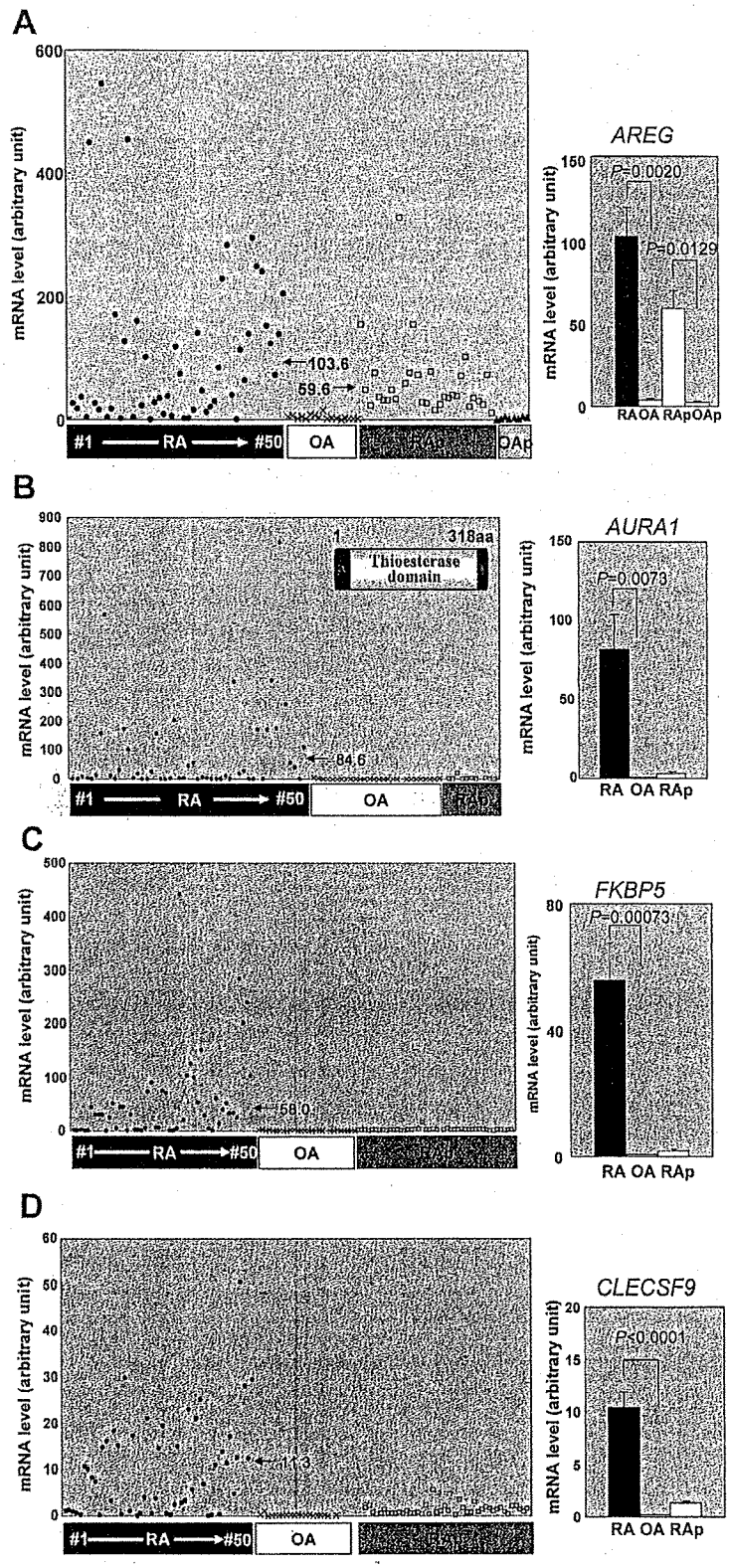

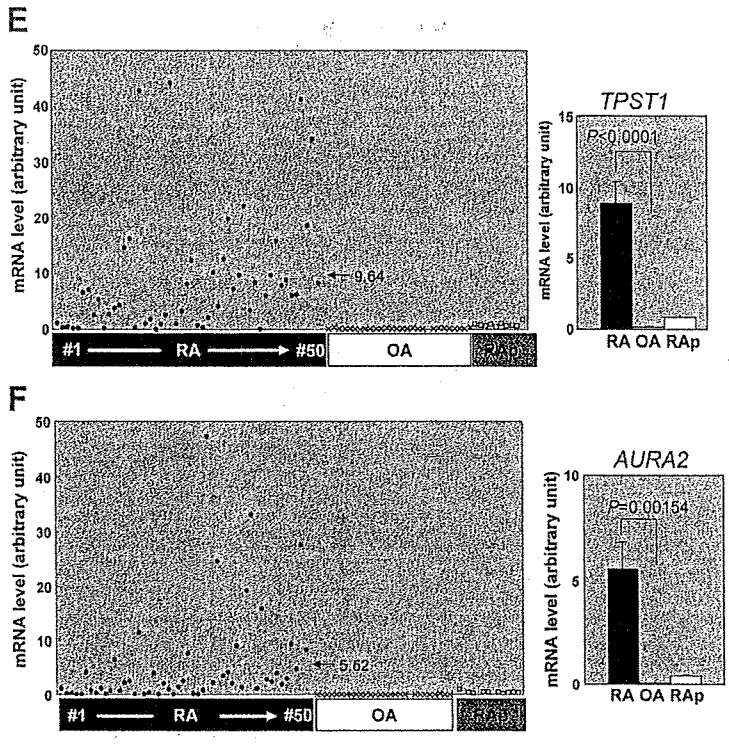

Figure 2. Expression levels of *AURA* genes in individual RA and OA patients. QRT–PCR analyses show that the mRNA levels of (A) *AREG*, (B) *AURA1*, (C) *FKBP5*, (D) *CLECSF9*, (E) *TPST1* and (F) *AURA2* are conspicuously upregulated in RA patient BMMC (and sometimes PBMC), while the BMMC and PBMC of OA patients show negligible upregulation. Expression levels in the BMMC for 50 RA patients (from #1 to 50) are arranged in the denoted order. The inset in (B) shows that the thioesterase domain occupies most of the Aura1 protein. The mean values of the samples analyzed in triplicate from each individual RA BMMC, RA PBMC, OA BMMC and OA PBMC are indicated by filled circles, open squares, x's, or filled triangles, respectively. The average values for the RA patient group are shown by the horizontal arrows. The bar graphs in the right panels show the average ± SE values of these measurements using the RA or OA BMMC or PBMC. All measurements are statistically significant when RA and OA are compared ($P < 0.01$).

AREG treatment upregulated the phosphorylated ERK1/2 expression levels much more strongly in the synoviocytes from RA2, RA3 and RA4 than in the synoviocytes of any of the OA patients. RA1 is an exception to this pattern as its limited phosphorylated ERK1/2 expression levels were similar to those in OA1–3. The AREG-induced upregulation of ERK1/2 phosphorylation was less apparent in the RA5 synovial cells because ERK1/2 was already activated in the absence of AREG.

Synoviolin plays a role in the synovial hyperplasia of RA by controlling the ERAD system.[10] To determine if the RA synovial cells have an abnormal ERAD system, we measured their levels of the ER stress proteins GRP78/BiP and GRP94, which protect cells from the stress-induced ER dysfunction that could lead to the accumulation of unfolded proteins.[33] We found that while the synovial cells of the RA and OA patients have similar levels of GRP78/BiP (Fig. 5B and D), the RA synoviocytes show enhanced levels of GRP94, irrespective of whether they have been stimulated with AREG. This suggests that at least part of the ER-stress responsive pathway, namely, that mediated by GRP94, is more activated in RA synoviocytes than in OA synoviocytes. Thus, the ERAD pathway does appear to be abnormally upregulated in RA synoviocytes. We confirmed by QRT–PCR that the BMMC and PBMC cells of RA patients RA1–5 show enhanced AREG mRNA levels, unlike the BMMC and PBMC of OA patients OA1–3 (Supplementary Figure S5A). Thus, chronic activation of AREG/EGFR signaling appears to be augmented in RA patients. Since AREG is expressed as transmembrane precursors that are cleaved in the extracellular domain to release soluble growth factor,[34] we speculated that the sera (PB) and bone marrow fluid (BM) of RA1–5 may show enhanced levels of cleaved AREG compared to the equivalent fluids of OA1–3. We tested this by enzyme-linked immunosorbent assay but found only one patient, RA2, showed levels of cleaved AREG that exceeded the detection level of the assay (Supplementary Figure S5B). Thus, it is not clear whether RA patients indeed secrete higher AREG levels than OA patients.

We also examined whether RA synoviocytes expressed higher synoviolin mRNA levels than OA synoviocytes in the presence or absence of AREG. However, we could not detect any significant differences between the RA and OA patients in this regard (Supplementary

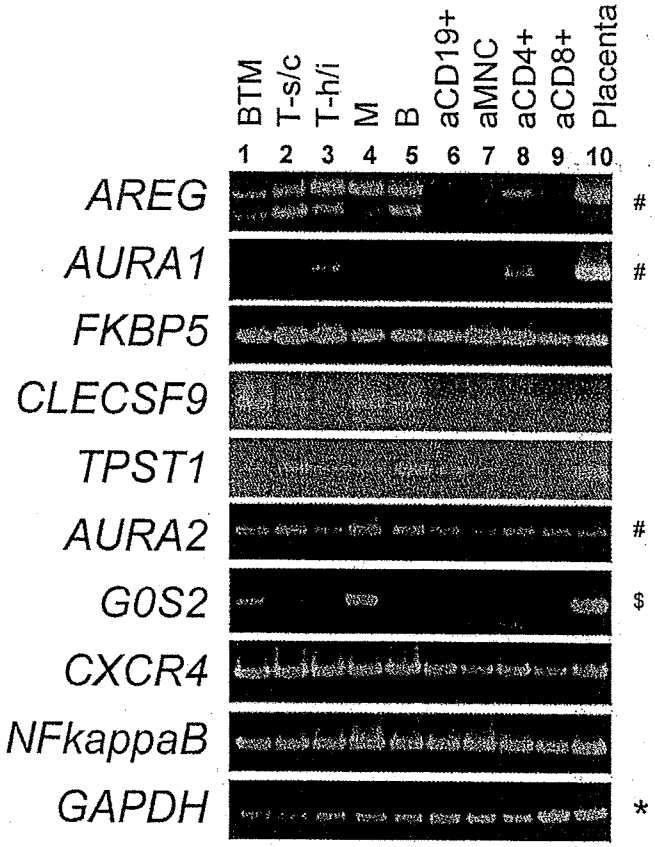

Figure 3. Determination by RT–PCR of the human blood cells that express *AREG*, *AURA1*, *FKBP5*, *CLECSF9*, *TPST1*, *AURA2*, *G0S2*, *CXCR4* and *NFκB*. RT–PCR was performed using the multiple tissue cDNA panel for human blood fractions (MTC, Clontech). *GAPDH* was also amplified as a loading control. PCR amplifications were conducted at 55°C and over 30 cycles except as indicated on the right of the panels: 55°C and 35 cycles (#), 55°C and 27 cycles (*) or 53°C and 25 cycles ($). Lane 1, mononuclear cells (B, T cells and monocytes). Lane 2, resting CD8+ cells (T-suppressor/cytotoxic cells).. Lane 3, resting CD4+ cells (T-helper/inducer). Lane 4, resting CD14+ cells (monocytes). Lane 5, resting CD19+ cells (B cells). Lane 6, activated mononuclear cells. Lane 7, activated CD4+ cells. Lane 8, activated CD8+ cells. Lane 9, activated CD19+ cells. Lane 10, human placenta control cDNA served as a DNA size marker.

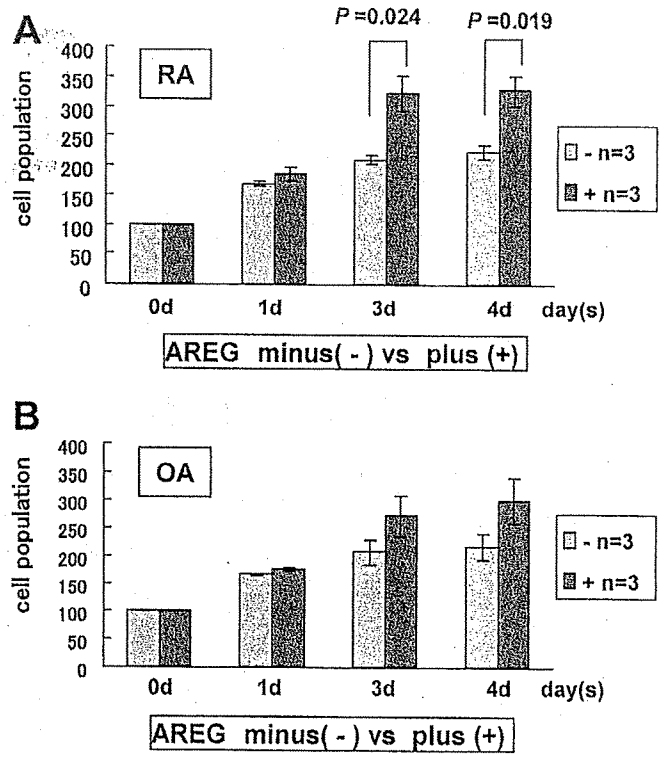

Figure 4. The effect of AREG on the proliferation of synoviocytes from RA and OA patients. The synovial cells from three RA patients (RA1, RA2 and RA3) (A) and three individual OA patients (OA1, OA2 and OA3) were counted on days 0, 1, 3 and 4 after incubation with or without AREG. The cell counts on days 1, 3 and 4 are expressed relative to 0 day. Statistically significant measurements are indicated ($P < 0.05$).

Figure S5C). It is not clear whether the synovial tissues of the patients would, like their cultured derivatives, show a similar lack of synoviolin upregulation.

4. Discussion

In this study, we report our comprehensive isolation of *AURA* genes that show augmented mRNA expression in the BMMC of RA patients as compared to their expression in OA patient BMMC (Fig. 1 and Table 1). Since RA patients suffer from defective central and peripheral B-cell tolerance checkpoints, and often display unusual immunoglobulin light chain repertoires that suggest impaired secondary recombination regulation,[18] we had expected that many immune response genes would be identified as *AURA* genes. Indeed, >10% of the *AURA* genes are directly related to immune responses; moreover, while the other *AURA* genes may seem at first glance to be unrelated to immune responses, many of these can also be linked to immune responses (Table 1). QRT–PCR analysis on individual patient samples revealed that the *AURA* genes discussed below are significantly increased in the BMMC of many of the 50 RA patients we tested (Fig. 2). Thus, the identification of these genes may help us to understand the pathogenesis of RA.

FKBP5, one of the cellular receptors for the immunosuppressant FK506, was expressed at higher mRNA levels in many RA patients than in the OA patients; this was true for the BMMC of the RA patients but not for their PBMC (Fig. 2C). FK506 has been suggested to be an effective drug for reducing the pain associated with RA.[35] This is because it can suppress inflammation by inhibiting the production by synovial cells of prostaglandin E2; it does so by suppressing the IL-1β production by leukocytes.[36] The enhanced FKBP5 expression in RA BMMC is not due to FK506 treatment since at the time of this study, treatment with FK506

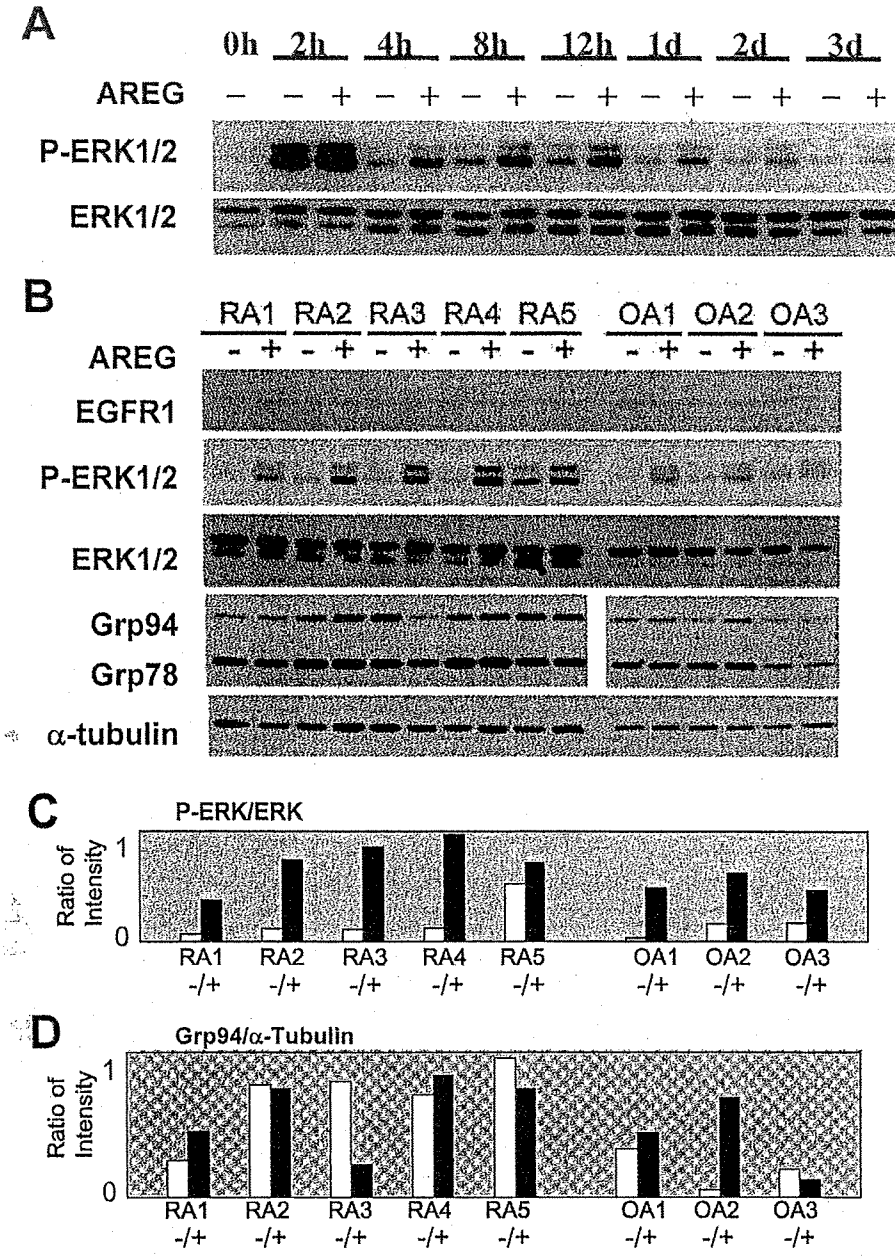

Figure 5. Western blot analysis of RA and OA synovial cells incubated in the presence or absence of AREG. (A) Expression levels of ERK1/2 and its phospho-form (P-ERK1/2) that is phosphorylated at Thr202 and Tyr204. Pooled synovial cells from five RA patients were incubated with (100 ng/ml) or without AREG for varying periods ranging from 0 h to 3 days. (B) Expression levels of EGFR1, ERK1/2, P-ERK1/2, Grp94, Grp78 and synoviolin in synovial cells from individual RA and OA patients that were incubated with or without AREG (100 ng/ml) for 8 h. Alpha-tubulin served as a loading control. (C) Relative optical densities of the western blot bands in (B) to determine P-ERK1/2 expression relative to ERK1/2 expression. (D) Relative optical densities of the western blot bands in (B) to determine Grp94 expression relative to alpha-tubulin expression.

was not permitted in Japan; consequently, none of the patients tested here have ever received FK506. In addition, the enhanced FKBP5 expression by RA BMMC does not correlate with therapeutic treatment using steroids. It remains possible, however, that the increased FKBP5 mRNA levels in the BMMC of RA patients may be due to treatment with other drugs. Alternatively, it may reflect genuine and spontaneous pathological events. Nevertheless, regardless of the cause of its elevated expression, the augmented FKBP expression may strongly inhibit the phosphatase activity of calcineurin, which could increase the dephosphorylation and thus inactivation of various substrates, including the NFAT family proteins and cytokines that are required for the expression of immunoregulatory molecules.

TPST1 mediates tyrosine sulfation within the trans-Golgi system, which affects 1% of all tyrosines in eukaryotic cells. It has been previously suggested that this post-translational modification may play an

important role in the pathogenesis of autoimmune diseases because it regulates mononuclear cell function at various stages of the immune response by enhancing interactions between ligands and receptors.[37] Notably, of the 62 identified target proteins of tyrosine sulfation, nine are cell adhesion molecules and chemokine receptors, which are both central players in leukocyte trafficking. Thus, the augmented expression of *TPST1* in RA patients may elevate the sulfation of crucial tyrosine residues in chemokine receptors that could constitutively increase their binding affinities with their ligands (e.g. the binding of CXCL12–CXCR4).

CLECSF9 belongs to the macrophage-inducible C-type lectin that serves multiple functions by recognizing carbohydrate chains; it plays important roles in macrophage function. Notably, a C-type lectin called DC-specific intercellular adhesion molecule 3-grabbing non-integrin is also highly expressed by macrophages in the synovium of RA patients.[38] However, the HH mRNA expression of macrophage-inducible C-type lectins is strongly induced in response to several inflammatory stimuli. Thus, the augmented expression of *CLECSF9* in the BMMC of RA patients may simply be due to the inflammation in the joint.

Unlike *FKBP5* and *TPST1* genes, the mRNA levels of G0S2, CXCR4 and NF-κB are increased in both the BMMC and PBMC of RA patients (Fig. 2 and Supplementary Figure S3). We previously showed that the PBMC of both systemic lupus erythematosus (SLE) patients and healthy young females express enhanced levels of *G0S2* mRNA.[26] Thus, G0S2 may not actually be involved in the pathogenesis of RA. With regard to the chemokine receptor CXCR4, it was also identified as a inflammation-related gene that is upregulated in synovial cells of patients with pigmented villonodular synovitis (PVNS), which is a joint problem that usually affects the hip or knee and involves the lining of the joint becoming swollen and growing.[8] The enhanced tyrosine sulfation of CXCR4 by augmented TPST1 activity, as described above, may also activate CXCR4, thereby elevating the ability of the CXCR4 ligand to induce the migration of bone marrow cells that could enhance the growth of synovial cells.[39] CXCR4 expression is also upregulated in the spinal cord of animals with experimental autoimmune encephalomyelitis, which is an animal model of autoimmune central nervous system inflammation.[40] With regard to NF-κB, this molecule along with the receptor activator of NF-κB (RANK) and its ligand RANKL have been found to play pivotal roles in the pathophysiological process of RA.[41] Thus, the increased mRNA levels of NF-κB in both the BMMC and PBMC of RA patients may contribute to the bone destruction mediated by activated NF-κB signaling pathway.[42]

AURA1 encodes a novel protein that is similar to thioesterase. Since the thioesterase homologs are widespread, functions of thioesterase vary in the human genome.[43] Thus, the physiological function of *AURA1* remains unknown. A possible role that it could play in RA pathogenesis is suggested by the following observations. First, the stable overexpression of acyl-CoA thioesterase III in human and murine T-cell lines increased both peroxisome numbers and lipid droplet formation, which suggests that it participates in the metabolic regulation of peroxisome proliferation in T cells.[44] Second, altered immune responsiveness is observed in mice deficient in palmitoyl protein thioesterase (PPT1) gene that is mutated in infantile neuronal ceroid lipofuscinosis.[45] Third, $CD4^+$ T cells are the prime mediators of RA in a mouse model SKG strain,[46] and *AURA1* expression is detected predominantly in resting and activated $CD4^+$ T cells (Fig. 3).

AREG is not directly related to immune responses but of all the genes examined, it showed the most conspicuously enhanced expression in both the BMMC and PBMC of many RA patients (Fig. 2A). We also found that the synovial cells of RA patients showed higher sensitivity to AREG, in terms of proliferation, than those of OA patients (Fig. 4). This is not due to augmented expression of EFGR (Fig. 5B, uppermost pane), but due to elevated activation of EGFR signaling pathway because the phosphorylation of ERK1/2 was more enhanced in AREG-treated RA patient synovial cells than that of AREG-treated OA patient synovial cells (Fig. 5). We here present a working hypothesis to explain how augmented AREG expression in BMMC and PBMC of RA patients and subsequent activation of EGFR signaling pathway lead to hyperproliferation of synovial cells in the joints of the RA patients (Fig. 6). Namely, this enhanced phosphorylation of ERK1/2 elevates the expression of many downstream target genes, which may also require the activation of the ERAD system. [12] Given that the Ets-binding site (EBS) of the proximal promoter of the synoviolin gene is responsible for its expression,[47] and that EBS-carrying genes are also activated by signaling events from the ERK pathway,[48] it is possible that the enhanced activation of EGFR signaling induced by AREG may directly activate the expression of synoviolin as well as that of other genes, thereby inducing the hyperproliferation of synovial cells. Thus, it is possible that the ERAD system in RA patients is hyperactivated by synoviolin because of augmented AREG expression in blood cells, possibly in the macrophages that occur in the vicinity of the synovial cells of RA patients, releasing augmented amount of AREG. This hypothesis should be tested more rigourously *in vivo* in the future because the experiments using the isolated synoviocyte cells in tissue culture medium may display distinct response to AREG. Likewise, examination of other EGF family proteins *in vivo* can also be interesting future subjects.